ULTRASTRUCTURE OF PORCINE TRICHOMONADS FROM CULTURE

by

James Willis Townsend

A Dissertation Submitted to the

Graduate Faculty in Partial Fulfillment of

The Requirements for the Degree of

DOCTOR OF PHILOSOPHY

Major Subject: Zoology (Parasitology)

Approved:

Signature was redacted for privacy.

In Charge of Major Work

Signature was redacted for privacy.

Head of Major Department

Signature was redacted for privacy.

Dean of Graduate College

Iowa State University
Ames, Iowa

1970

TABLE OF CONTENTS

INTRODUCTION

Trichomonads have been reported from the nasal cavity, stomach, small intestine, caecum and large intestine of swine. Hibler et al. (1960) noted the similarities between the nasal and the gastric forms and considered both of them to be Trichomonas suis. Morphological similarities between the nasal trichomonad and Trichomonas foetus (Riedmüller) were observed by Buttrey (1956).

Doran (1957) reported that the caecal trichomonad of swine differed physiologically from the nasal trichomonad and T. foetus. He found T. foetus and the trichomonad in the nose to be very similar, differing only in lactose and raffinose utilization. Doran (1959) speculated that the nasal trichomonad might be a highly adapted strain of T. foetus.

Similarities of serological reactions to T. foetus and T. suis have been reported by Kerr (1958). Results of an opposite nature were reported by Sanborn (1955).

Variable results have also been obtained in attempts to show cross-infection capabilities. Switzer (1951a) reported T. suis capable of infecting the genital tract of cows. This report was confirmed by Fitzgerald et al. (1958) who noted symptoms similar to those produced by T. foetus. Experiments by Hammond and Leidl (1957) gave similar results. Kerr (1958) found inoculations of T. foetus to be incapable of producing infections in the vagina of sows. Shaw and Buttrey (1958) found differences in the abilities of T. foetus and the nasal, stomach and caecal forms of swine trichomonads to establish infections in the digestive tracts of chickens when inoculated via the oral cavity.

Thus, the taxonomic relationships of the porcine trichomonads to each other and to T. foetus are not understood precisely at this time. Further studies are necessary, especially in regard to their ultrastructure. A comparison of the ultrastructure of the various trichomonads should provide additional information and aid in our understanding of these organisms from swine and cattle.

The purpose of this investigation is to determine and analyze the ultrastructure of the nasal and the stomach trichomonads from swine. Since Simpson and White (1964) have studied the ultrastructure of T. foetus, it will be possible to compare the results from the present study of the porcine trichomonads with those already reported for T. foetus. This comparison might indicate areas of similarity and difference among these organisms. If our taxonomic scheme for the trichomonads is to reflect evolutionary relationships, we must assume that closely related organisms will be highly similar in most, if not all, traits. Therefore, it is reasonable to assume that closely related organisms would share many similarities of ultrastructure.

LITERATURE REVIEW

At least three species of trichomonads have been described from swine. The description by Gruby and Delafond (1843) of a protozoan from the stomach of swine appears to be the earliest report of porcine trichomonads. On the basis of their vague description of this organism, Davaine (1877) named it Trichomonas suis.

Kunstler (1888) reported trichomonads in the intestine of swine and in the vagina of cattle. Of 33 market pigs in China, Kessel (1928a,b) found 11 to be harboring trichomonads in their intestines. He reported that in eight pigs, the trichomonads possessed three anterior flagella, while those trichomonads in the other three pigs had four anterior flagella. It is possible that, on the basis of work reported by Hibler et al. (1960), these latter organisms may have been Trichomonas buttreyi. Frye and Meleney (1932) found 47 of 63 swine harbored intestinal trichomonads. Large numbers of trichomonads were reported from the caecum of swine by Brumpt (1936).

Küst (1936) found trichomonads resembling T. foetus in the reproductive tract of one sow and aborted pig foetuses. This report could not be confirmed by McNutt et al. (1939) in their examination of 289 Iowa sows. They could find no trichomonads in the vaginal tracts of any of the experimental animals. The organism found by Küst was speculated to have been T. foetus since bovine trichomoniasis is so common in Southern Germany where the incident occurred.

Buttrey (1956) reported great similarity between porcine nasal trichomonads and T. foetus of cattle. He also concluded that the caecal trichomonad of swine was a different species than the nasal trichomonad.

Hammond, Fitzgerald and Johnson (1957) reported the nasal trichomonad of swine to be similar to those found in the stomach, but distinct from the caecal trichomonad. Hibler et al. (1960) found trichomonads in the nasal cavity, stomach, small intestine and caecum of swine. An organism identified as T. suis was reported from all four sites. A new species, Trichomonas buttreyi was found in the caecum and in the small intestine. Another new species, Tritrichomonas rotunda was described from the caecum and appears to be the caecal trichomonad reported by Buttrey (1956). These results were in agreement with later reports by Randall (1960) and by Randall and Buttrey (1961). The observation by Switzer (1951a,b) that, upon continued cultivation there was no distinguishable morphological variation between the nasal trichomonad and T. suis tends to support the viewpoint that they are indeed one species.

From a review of the literature, it would appear that there are at least three porcine trichomonads. One form, T. suis, is a T. foetus-like organism which may inhabit the nasal cavity, stomach, small intestine, caecum and large intestine. Another species, T. rotunda, inhabits the caecum and the third species, T. buttreyi, may be found in the caecum and small intestine.

There have been no electron microscope studies of porcine trichomonads. The ultrastructure of Trichomonas muris has been studied by Anderson (1955), Anderson and Beams (1959, 1961) and by Osada (1962).

Chakraborty, Das Gupta and Ray (1961) reported on the ultrastructure of Trichomonas criceti. The ultrastructure of Trichomonas gallinae was described by Mattern, Honigberg and Daniel (1967). Studies of the fine structure of T. foetus were made by Inoki et al. (1961) and by Simpson and White (1964).

The human trichomonads have received much attention also. Trichomonas tenax was studied by Ohno (1960), and Pentatrichomonas hominis was studied by Honigberg, Mattern and Daniel (1968). Trichomonas vaginalis has been studied most intensively with results published by Inoki, Nakanishi and Nakabayashi (1959, 1960), Hashimoto et al. (1964), Nielsen and Ludvik (1964), Nielsen, Ludvik and Nielsen (1966), Smith and Stewart (1966) and Yeh, Huang and Lien (1966). While there have been other electron microscope studies of trichomonads, these appear to be the most significant reports.

MATERIALS AND METHODS

Two strains of porcine trichomonads in culture were used. Culture no. 1 (nasal strain) was originally isolated September 25, 1956, from the nose of a 40 lb castrated male pig on a farm near Vermillion, South Dakota. The nose and caecum were positive for trichomonads, but the presence of organisms in the stomach was uncertain. Culture no. 11 (stomach strain) was isolated July 9, 1957, from the stomach of a pig near Vermillion, South Dakota. The stomach was positive for trichomonads, while the caecum was negative.

Both strains were maintained in axenic culture in modified cysteine monohydrochloride-peptone-liver infusion-maltose medium (C.P.L.M.) (Table 1). The medium was dispensed in 8.5 ml amounts and autoclaved. Just prior to inoculation with trichomonads, 1.0 ml of heat inactivated fetal calf serum and 25,000 units of penicillin were added to each tube. The 0.5 ml inoculum contained approximately 20,000 organisms from a 48-hour culture, resulting in an initial population of 1,000 organisms in the 10 ml total volume of medium. The inoculated tubes were then incubated at 37°C.

Prior to fixation, each culture was inoculated into C.P.L.M. medium which had been modified by the omission of agar. After two subcultures in C.P.L.M. without agar, trichomonads in logarithmic growth phase were fixed for examination by light and electron microscopy. Logarithmic growth phase was confirmed by use of the bright-line improved Neubauer haemocytometer counting chamber.

Table 1. Modified cysteine monohydrochloride-peptone-liver infusion-maltose medium (Johnson, 1947 and Trussell, 1947)

Ingredient[a]	Quantity
Bacto peptone	16.0 g
Bacto agar	0.8 g
Cysteine monohydrochloride	1.2 g
Maltose	0.8 g
Difco liver infusion[b]	160 ml
Modified Ringer's solution[c]	480 ml
1.0 N NaOH	5.5 - 6.5 ml to pH 6.1±0.1

[a]All ingredients except 0.1 N NaOH were mixed and boiled for 5 min, then filtered through coarse filter paper. The medium was then titrated to pH 6.1±0.1 with the 0.1 N NaOH. After titration, 0.4 ml of 0.5% aqueous methylene blue was added.

[b]Difco liver infusion: Bacto dehydrated liver 62.5 g
Distilled water 1,000 ml
This mixture was heated to 50°C for one hour. The temperature was then raised to 80°C and the mixture filtered immediately through coarse filter paper. The filtrate was autoclaved and stored in the refrigerator.

[c]Modified Ringer's solution:

NaCl	6.0 g
$NaHCO_3$	0.1 g
$CaCl_2$	0.1 g
KCl	0.1 g
Distilled water	1,000 ml

Table 2. Phosphate-buffered glutaraldehyde fixative

A. Buffer: Mixture of 23 ml solution A and 67 ml solution B (final pH 7.1)
1. Solution A: $NaH_2PO_4 \cdot H_2O$ 2.76 g in 100 ml H_2O
2. Solution B: $Na_2HPO_4 \cdot 7H_2O$ 5.66 g in 100 ml H_2O

B. Fixative: Mixture of equal volumes of the following:
1. 5.0% glutaraldehyde in pH 7.1 buffer
2. 0.2 M sucrose solution

Light microscope observations were made on cultures fixed and stained by the following methods: (1) Bouin's fixative and Nie's protargol (Nie, 1950) and (2) Schaudinn's fixative and Heidenhain's iron haematoxylin. Specimens were fixed and stained on coverglasses, then mounted in Pro-Texx (Scientific Products Co.). The organisms were measured by means of an ocular micrometer.

Specimens were prepared for electron microscopy according to the following format:

1. Centrifugation for concentration at about 1,000 rpm for 15 min.
2. Fixation overnight at 4°C in phosphate-buffered 5% glutaraldehyde (Table 2).
3. Two rinses in phosphate-buffered 1% sucrose solution for 10 min each.
4. Post-fixation in 1% OsO_4 in phosphate-buffered sucrose solution for 30 min at room temperature.
5. Rinse in phosphate buffer (no sucrose) 2 times, 10 min each.
6. Dehydration in the following sequence:
    a. 50% ethanol, 5 min.
    b. 75% ethanol, 5 min.
    c. 85% ethanol, 5 min.
    d. 95% ethanol, 5 min.
    e. 100% ethanol, 2 times for 10 min each.
7. Clearing in propylene oxide (1,2-epoxypropane), 2 times for 10 min each.

8. Infiltration in 75% propylene oxide: 25% epon for 2 hrs.

9. Infiltration overnight in 50% propylene oxide: 50% epon, uncovered, to allow the propylene oxide to evaporate.

10. Embedding in 1:1 mixture of Epon A and Epon B (Table 3) and left at room temperature for 12 hrs.

11. Cured at 35°C for 12 hrs.

12. Cured at 45°C for 12 hrs.

13. Cured at 60°C for at least 24 hrs.

After steps 2 through 7 the organisms were concentrated by centrifugation at about 1,000 rpm for 10 min; after steps 8 and 9 they were centrifuged at about 1,000 rpm for 60 min.

The specimens were then sectioned at 60-100 millimicrons (mμ) with glass knives on a Sorvall MT-2 or a Reichert Om-U2 ultramicrotome. Sections were placed on uncoated 400 mesh copper grids, stained with methanolic uranyl acetate (Table 4) and lead citrate (Table 5). These preparations were then examined in an RCA model EMU3F electron microscope at 100Kv.

Table 3. Epon embedding medium

A. Epon A	
Epon 812 resin	62 ml
Dodecenyl succinic anhydride (DDSA)	100 ml
B. Epon B	
Epon 812 resin	100 ml
Nadic methyl anhydride	89 ml

After mixing equal volumes of Epon A and Epon B, Tris (dimethylaminomethyl) phenol (DMP-30) was added in the proportion of 1.5% - 2.0% as an accelerator.

Table 4. Staining procedure with methanolic uranyl acetate

Uranyl acetate	15.0 g
Absolute methanol (reagent)	100 ml

Grids to be stained were immersed in a drop of stain on a spot plate which was set in absolute methanol inside a covered petri dish to avoid evaporation of methanol from the stain. Staining time was 5 min, followed by washing in 3 separate beakers of absolute methanol, 15 dips each.

Table 5. Lead citrate stain (Venable and Coggeshall, 1965)

Lead citrate	0.02 g
Distilled water	10 ml
10 N NaOH	0.1 ml

The above ingredients were placed in a screw-top culture tube and shaken vigorously to dissolve the lead citrate. Grids previously stained with methanolic uranyl acetate were then immersed in lead citrate on a spot plate for 5 min. After staining, the grids were washed by dipping them 15 times in each of 3 beakers of boiled (CO_2-free) distilled water.

RESULTS

Nasal Trichomonad

Light microscopy

Size and form This trichomonad was characteristically pyriform or oval in shape. After prolonged culture, the form became more generally rotund with less variation than was seen in smears from the original host. The measurements of length and width of 50 specimens from the original host and another 50 specimens from the 1969 C.P.L.M. culture (subculture no. 637) are given in Table 6.

Table 6. Measurements of body size of nasal trichomonads

Source (Number measured)	Stain	Length[a] (μ)	Width[a] (μ)
Host (50)	Haematoxylin	10.0 ± 1.66 (6.6-14.1)	4.8 ± 0.93 (3.6-7.2)
Host (50)	Protargol	10.3 ± 2.10 (6.6-17.8)	4.3 ± 0.84 (2.8-6.2)
Subculture no. 637 (50)	Haematoxylin	13.4 ± 1.33 (10.8-16.9)	6.4 ± 1.02 (4.8-8.9)
Subculture no. 637 (50)	Protargol	13.2 ± 1.86 (9.6-17.1)	6.2 ± 1.38 (4.1-8.4)

[a]Measurements are given as: mean ± standard deviation, with ranges in parentheses.

Blepharoplast This structure was measured only from haematoxylin preparations because of its poor affinity for the protargol stain.

Preparations from the original host had a blepharoplast measuring 0.9μ (0.7-1.1) while organisms from the culture had a measurement of 0.8μ (0.5-1.2) for this organelle. The karyomastigont structures (flagella, undulating membrane, costa, axostyle, nucleus and parabasal body) originated in the general area of the blepharoplast.

Nucleus This ovoid structure was located in the anterior 1/2 of the organism. The nucleus was measured in haematoxylin-stained specimens and was found to be 4.8μ (4.2-5.7) long and 2.2μ (1.7-2.7) wide in the trichomonads from the host. The nuclei of organisms from culture measured 4.6μ (3.0-5.6) in length and 2.8μ (2.3-3.8) in width. Measurements were made more difficult by the presence of the nuclear cloud which obscured the margins of the nucleus. Coarse basophilic granules interpreted as chromatin were seen scattered throughout the nucleus in haematoxylin preparations. Some nuclei possessed a centrally located endosome within a localized, lightly staining area.

Parabasal body In protargol-stained specimens, this structure appeared to originate in the blepharoplast region and extended posteriorly along the right dorsal lateral aspect of the nucleus. The parabasal body was apparently a single finger-like structure. Its length was 2.8μ (2.3-3.1) in smears from the original host, and 3.0μ (2.6-3.3) in the cultured organisms. Widths were 0.9μ (0.7-1.0) and 1.0μ (0.7-1.2), respectively.

Axostyle This structure extended the full length of the organism, originating in the blepharoplast region and terminating in a projecting tip in the posterior region. The anterior 1/4 to 1/3 of the axostyle was modified as a bulbous or spoon-shaped capitulum and was associated with the ventral side of the nucleus. Posterior to the nucleus, the axostyle had a diameter of 0.9μ (0.7-1.2) in organisms from the host and 0.9μ (0.8-1.2) in those from culture. Measurements were made from haematoxylin preparations. Posteriorly, in the region of its projection from the cytoplasm, the axostyle was surrounded by a chromatic ring. The chromatic ring was strongly basophilic. The conical tip of the axostyle projected from the cytoplasm 2.1μ (1.0-2.9) in organisms from the host and 2.6μ (1.2-3.4) in organisms from culture.

Costa Arising in the blepharoplast region, the costa was directed posteriorly along the base of the undulating membrane to a common posterior terminus with the undulating membrane. The costa stained very heavily with both protargol and haematoxylin. It appeared to be slightly thicker in the middle 1/3 of the organism than at either extremity. Occasionally, subcostal granules could be seen in both protargol and haematoxylin preparations.

Undulating membrane Between the recurrent flagellum and the body of the organism was the fin-like undulating membrane. Its elevation from the body of the trichomonad reached a maximum height of 1.3μ (1.0-1.5) in organisms from the host, and 1.2μ (0.8-1.8) in the cultured forms. The undulating membrane arose in the region of the blepharoplast

and terminated with the costa in the posterior 1/4 of the trichomonad. A total of four to six subequal folds of the undulating membrane were seen in all these specimens. The fact that the undulating membrane had a greater linear dimension than the underlying costa was indicated by the presence of the subequal folds, since the undulating membrane and the costa originate and terminate together. A marginal filament was detected in both protargol and haematoxylin stained preparations; it coursed along the outer margin of the undulating membrane just proximal to the recurrent flagellum.

Anterior flagella Three anterior flagella originated in the blepharoplast region and were directed anteriorly. Two of the three were of approximately equal length with the shortest ranging 3.0-5.0μ less. Measurements of the longest anterior flagella were made from protargol preparations. The anterior flagella of organisms from the host averaged 12.6μ (10.4-14.4) while those from culture averaged 11.7μ (10.3-13.2). The anterior flagella often terminated in small bulb-like modifications.

Recurrent flagellum This structure originated in the blepharoplast region and proceeded posteriorly along the outer margin of the undulating membrane. From the point of termination of the undulating membrane, the recurrent flagellum extended as an independent trailing flagellum. The length of the trailing flagellum varied widely in both groups of trichomonads. Lengths of 10.7μ (3.6-12.1) in organisms from the host and 10.9μ (4.1-13.6) in those from the culture were recorded.

Electron microscopy

Nucleus The nucleus of these organisms was enclosed in a double layer of unit membrane (Figs. 1, 2, 4 and 5). Surrounding the nucleus were two concentric layers of rough endoplasmic reticulum (Figs. 1 and 4) bearing ribosomal particles of 13 millimicrons (mμ) diameter. The cisternal space of the rough endoplasmic reticulum measured 33 mμ. Nucleolar areas were seen in the nucleus (Figs. 1, 3 and 5).

Blepharoplast The structure referred to as a blepharoplast by light microscopists appears to be the kinetosome complex as described by electron microscopists. Its ultrastructure will be discussed in the descriptions of the anterior and recurrent flagella.

Parabasal body The parabasal body was composed of flattened cisternal elements of smooth endoplasmic reticulum (Figs. 2, 6, 7, 8 and 9). These cisternae were 19mμ diameter. Sections made near the periphery of the parabasal body showed many of these vesicles to contain darkly staining material (Fig. 8).

Axostyle The axostyle proved to be a complex of microtubular elements of 27mμ diameter arranged in a stockade-like pattern. Cross sections of the posterior portion of the axostyle showed it to be tubular (Figs. 10 and 11). There appeared to be no limiting membrane around the axostyle. In the anterior portion of the organism, the stockade-like pattern of axostylar microtubules were arranged in a sheet. This sheet of microtubules enclosed the kinetosomes (blepharoplast) of

the anterior and recurrent flagella, the nucleus and the parabasal body (Figs. 6, 8, 13, and 14). In some organisms, there were two axostyles which were interlocked (Fig. 18).

Endoaxostylar granules These structures were membrane-limited and their contents appeared homogeneous (Figs. 4, 5, 7, 12, 13, 14 and 15). Their structure was indistinguishable from that of the subcostal granules (Fig. 3). Maximum diameter of the endoaxostylar granules was 0.7μ. The endoaxostylar granules were found only in sections of the anterior portion of the organism in the axostylar capitulum. There was a consistent association of the endoaxostylar granules with one edge of the sheet-like axostylar capitulum (Figs. 4, 5, 14, 15 and 17). Some sections showed a layer of rough endoplasmic reticulum associated with these granules (Fig. 20).

Paraxostylar granules Predominating in the region of the organism posterior to the nucleus and associated with the axostyle were the paraxostylar granules. They were membrane-limited and their contents showed a distinct lamellar nature (Figs. 1, 2, 4, 5, 11, 15, 17 and 20). There seemed to be no consistency in the number of lamellae per granule. Diameters of the paraxostylar granules were on the order of 1.0μ.

Pelta An organelle which had not been reported from light microscope observations is the pelta. The exact nature of this structure presents a problem of interpretation. Essentially, it appears to be a

sheet of microtubules (Figs. 12, 13 and 21) of 24mμ diameter. These microtubules were parallel to the microtubules of the axostylar capitulum and lay within the area enclosed by the capitulum (Figs. 12, 13, 14, 16, 19, 21, 22 and 23). The pelta was directed anteriorly with a flexure that curved around the flagellar kinetosomes (Figs. 13, 16 and 21).

Costa The costa originated in the region of the kinetosome of the recurrent flagellum (Figs. 1, 12, 13, 16, 21, 22, 23 and 24). A definite periodic structure was seen in longitudinal section (Figs. 20, 21 and 22). There were alternating dark and light bands each on the order of 20mμ. The dark band was composed of three narrow bands separated by 10mμ (Fig. 20). In favorable longitudinal sections, a sheath could be seen (Figs. 22, 25 and 26). Transverse sections of the costa showed it to be homogeneous in composition, with a 300mμ width. The paracostal sheath was composed of very fine microtubules of 5mμ diameter (Figs. 27, 28 and 29). The costa was always closely associated with the undulating membrane.

Subcostal granules These granules were of relatively low contrast and were membrane-limited (Figs. 2, 20, 29 and 31). Their maximum diameters were on the order of 700mμ and their contents were homogeneous. In longitudinal sections of the costa, the subcostal granules were seen to parallel the costa on the side opposite the undulating membrane (Figs. 20, 31 and 32).

Undulating membrane The undulating membrane appeared to be a specialized extension of the cytoplasm which was closely adherent to the recurrent flagellum (Figs. 2, 5, 8, 14, 20, 21, 23, 25, 28, 29, 30 and 32). In favorable transverse sections, the undulating membrane was seen to contain microtubular elements with diameters of 20mμ (arrows, Fig. 30). These microtubular elements were arranged in four rows which were oriented vertically to the recurrent flagellum (Figs. 5, 30 and 32). No distinct structural connection between the undulating membrane and the recurrent flagellum could be resolved, but some micrographs showed a rather indistinct cloudy area between them (Figs. 4, 30 and 32). The undulating membrane was separated from the recurrent flagellum by a distance of 8mμ.

Anterior flagella The kinetosomes of the anterior flagella were composed of 9 sets of 3 fibrils each with diameters of the fibrils being 19mμ. These triplet structures were arranged in a cylindrical pattern with their axes skewed slightly (Figs. 13, 19, 21, 24 and 33). The centers of the kinetosomes contained electron-dense areas (Fig. 33). Associated with the kinetosomes were rootlets which appeared to connect the kinetosomes into a kinetosome network. The rootlet of kinetosome no. 2 arose in the region of the pelta-axostylar junction (Figs. 16 and 21). Rootlets of the remaining two anterior flagella apparently served as connections with the other flagella-elements (Figs. 13, 19 and 21). The flagella showed the standard 9+2 configuration of 9 peripheral double fibrils of 16mμ diameter and 2 central single fibrils of 20mμ diameter. Sections of the terminal portion of the flagellum showed

the reduction of the peripheral double fibrils to single fibrils without the loss of the central fibrils (Figs. 10 and 34).

Recurrent flagellum The kinetosome of the recurrent flagellum was oriented at right angles to the kinetosomes of the anterior flagella (Figs. 13 and 24). In addition, the kinetosome of the recurrent flagellum was intimately associated with the anterior terminus of the costa (Figs. 22, 23 and 24). The structure of the kinetosome of the recurrent flagellum was identical with that of the anterior flagella (Figs. 4 and 11). However, the recurrent flagellum had a greater amount of cytoplasm surrounding the fibrils than did the anterior flagella. The fibrils of the recurrent flagellum always appeared displaced toward the side of the flagellum lateral to the undulating membrane (Figs. 2, 3, 4, 5, 8, 14, 21, 23, 25, 29, 30 and 32).

Stomach Trichomonad

Light microscopy

Size and form The stomach strain was oval or pyriform in shape. As in the case of the nasal strain, prolonged culture gave rise to a higher proportion of more rotund individuals. Measurements of the length and width of the stomach strain were made on specimens from the original host, organisms from the 2nd subculture, and from the 636th subculture. Due to the low numbers of organisms in the smears from the stomach of the original host, only 25 measurements were made from each of the protargol and haematoxylin preparations. The measurements of lengths and widths of the stomach trichomonads are given in Table 7.

Table 7. Measurements of body size of stomach trichomonads

Source (Number measured)	Stain	Length[a] (μ)	Width[a] (μ)
Host (25)	Haematoxylin	7.9 ± 1.24 (6.0-10.6)	5.5 ± 2.27 (4.2-6.9)
Host (25)	Protargol	8.1 ± 1.85 (5.6-12.2)	4.8 ± 1.33 (2.1-6.6)
Subculture no.2 (50)	Haematoxylin	11.6± 1.50 (7.5-14.1)	5.3 ± 1.40 (2.8-5.6)
Subculture no.2 (50)	Protargol	10.8± 1.17 (8.5-13.6)	4.2 ± 0.71 (2.8-5.6)
Subculture no.636 (50)	Haematoxylin	12.0± 1.91 (8.1-17.9)	6.1 ± 0.96 (4.0-8.2)
Subculture no.636 (50)	Protargol	11.3± 1.64 (7.3-16.7)	5.7 ± 1.12 (2.0-6.9)

[a]Measurements are given as: mean ± standard deviation, with ranges in parentheses.

Blepharoplast Haematoxylin preparations were used for the study of this structure. The blepharoplast measured 1.0μ in diameter (0.8-1.2) in organisms from the original host, 0.9μ (0.8-1.1) in organisms from subculture no. 2 and 0.9μ (0.5-1.4) in organisms from subculture no. 636. The mastigont structures originated in the area of the blepharoplast.

Nucleus In these organisms, the nucleus was ovoid and located in the anterior 1/2 of the organism in close association with the dorsal side of the axostylar capitulum. The nucleus measured 2.8μ in length (2.4-3.0) and 2.1μ in width (1.7-2.4). Subculture no. 2 had organisms with nuclear lengths averaging 4.9μ (3.5-5.8) and widths averaging 2.7μ

(1.9-3.6). Subculture no. 636 nuclear measurements were 4.9μ (3.8-6.0) by 2.9μ (2.4-3.6). The measurements were all made from haematoxylin preparations. A distinct nuclear cloud obscured the nucleus and made measurements somewhat more difficult. Basophilic granules were seen scattered throughout the nucleus in haematoxylin preparations and were interpreted as concentrations of chromatin. A central endosome was noted haematoxylin-stained organisms, and it was usually located within a lightly staining halo.

Parabasal body Protargol preparations showed the parabasal body to be an oblong structure originating in the region of the blepharoplast and extending along the right dorsal lateral aspect of the nucleus. Trichomonads from the host had parabasal bodies averaging 2.1μ in length (1.6-3.2) and 0.6μ in width (0.4-1.0). Subculture no. 2 had measurements of 3.5μ (2.8-4.1) by 0.8μ (0.6-1.1). The parabasal body averages for subculture no. 636 were 3.2μ (2.4-3.8) in length and 0.9μ (0.4-1.3) in width.

Axostyle Originating in the blepharoplast area, the axostyle extended the full length of the organism and terminated in a projecting tip at the posterior of the organism. The anterior 1/4 to 1/3 of the axostyle was modified as a bulbous or spoon-shaped capitulum. The capitulum was associated with the ventral side of the nucleus. At the posterior limit of the nucleus, the axostyle made the transition to a rod-like shape. In haematoxylin preparations, axostylar diameters posterior to the nucleus were 0.8μ (0.5-1.2) for trichomonads from the

original host, 0.8μ (0.6-1.1) for subculture no. 2 and 0.9μ (0.8-1.1) for subculture no. 636. At the point of its projection from the cytoplasm in the posterior region of the organism, the axostyle was surrounded by a chromatic ring. In protargol preparations, the chromatic ring appeared as a series of rings or as a tightly coiled spiral surrounding the axostyle. In haematoxylin-stained specimens, it had a more granular appearance and stained quite heavily. The axostylar tip projected 1.9μ (0.9-2.6) from the body of trichomonads isolated from the original host. Projections of 2.0μ (1.1-3.1) were found in subculture no. 2 and 2.4μ (1.0-3.5) in subculture no. 636. Endoaxostylar granules and paraxostylar granules were abundant in all three groups. The endoaxostylar granules appeared to be in a single row and had diameters of 1.2μ (1.0-1.5) in organisms from the original host, 1.4μ (1.1-1.7) in subculture no. 2 and 1.4μ (1.0-1.6) in subculture no. 636. Endoaxostylar granules were generally restricted to the region of the capitulum, while paraxostylar granules were found at all levels, but they predominated in the region posterior to the capitulum. Paraxostylar granules measured 1.0μ (0.8-1.2) in organisms from the original host, 1.1μ (0.8-1.4) in organisms from subculture no. 2 and 1.1μ (0.9-1.5) from subculture no. 636. Paraxostylar granules showed no linear regularity of position similar to that of the endoaxostylar granules.

Costa This organelle arose in the blepharoplast region and terminated at the posterior limit of the undulating membrane. Along

its course, it was located at the base of the undulating membrane, and stained heavily with both protargol and haematoxylin. The costa appeared thicker in the middle 1/3 of the organism than at either end. Protargol and haematoxylin preparations revealed the presence of subcostal granules of 1.0μ (0.7-1.2) in organisms from the original host, 0.9μ (0.7-1.0) in subculture no. 2 and 1.0μ (0.6-1.2) in subculture no. 636.

Undulating membrane Characteristically, this structure was a fin-like extension of the cytoplasm along the dorsal surface of the organism. It extended from the blepharoplast region to the posterior terminus of the costa in the posterior 1/4 of the organism. The undulating membrane had the recurrent flagellum lying along its outer margin. The maximum height of the undulating membrane was 1.1μ (0.6-1.5) in organisms from the host, 1.0μ (0.5-1.4) in subculture no. 2 and 1.5μ (1.4-1.9) in subculture no. 636 as measured in protargol preparations. The undulating membrane showed a marginal filament when stained with protargol or haematoxylin. The marginal filament was located just proximal to the recurrent flagellum. There were four to six subequal folds of the undulating membrane seen in all specimens. This folding apparently is necessitated by differences in linear dimension of the costa and the recurrent flagellum, both of which are associated with the undulating membrane.

Anterior flagella Originating in the blepharoplast region, the three anterior flagella were subequal. Measurements of the longest

flagellum of individual organisms from protargol preparations were 10.7μ (7.6-13.8) in organisms from the original host, 11.5μ (8.9-15.0) in subculture no. 2 and 11.0μ (8.9-15.0) in subculture no. 636. The second anterior flagellum was of approximately the same length as the longest, with the third anterior flagellum being 2-6μ shorter than the longest. In protargol preparations, the anterior flagella often ended in terminal knobs.

Recurrent flagellum This structure also originated in the blepharoplast region. It extended along the outer margin of the undulating membrane to the terminus of the undulating membrane in the posterior 1/4 of the organism. The recurrent flagellum then extended from the body of the trichomonad as an independent trailing flagellum whose length varied from 8.4μ (2.5-9.6) in organisms from the original host, to 8.9μ (3.1-9.7) in subculture no. 2 and 10.8μ (4.3-12.4) in subculture no. 636 as measured in protargol preparations.

Electron microscopy

Nucleus The nucleus of the stomach trichomonad was limited by a double layer of unit membrane (Figs. 35 and 36). Two concentric layers of rough endoplasmic reticulum surrounded the nucleus (Fig. 35). The cisternal spaces of the rough endoplasmic reticulum measured 20mμ in width, and the ribosomes on the rough endoplasmic reticulum had a diameter of 12mμ (Fig. 35). Nucleolar areas were seen in the nucleus (Figs. 35 and 37). The maximum dimension of any nucleolus was 1.0μ (Fig. 35).

Blepharoplast The structure identified as a blepharoplast by light microscopy appears to be the kinetosome complex of the anterior and recurrent flagella. Thus, the ultrastructure of the blepharoplast will be considered in the descriptions of the anterior and recurrent flagella.

Parabasal body This organelle was composed of flattened cisternal elements of smooth endoplasmic reticulum which were swollen along their periphery and associated with numerous small vesicles (Figs. 36 and 38). The cisternae were 12mμ wide and the associated vesicles had a diameter of 37mμ (Figs. 36 and 38). The vesicles often were seen to have darkly staining contents (Fig. 38).

Axostyle The axostyle was a microtubular complex arranged in a stockade-like pattern. The diameter of the microtubules was 29mμ (Figs. 39 and 40). In the capitulum area of the axostyle, the stockade-like arrangement of microtubules was in a sheet (Figs. 36 and 41) which enclosed the nucleus, parabasal body and endoaxostylar granules. Posterior to the nucleus, the axostylar microtubules were in a cylindrical orientation (Figs. 39 and 40) with no limiting membrane. Some organisms with two axostyles were found (Fig. 42) and in these cases the axostyles were interlocked.

Endoaxostylar granules These structures were found only in the capitulum region of the axostyle (Figs. 36 and 41). They were membrane-limited and had a homogeneous matrix. The maximum diameter of the

endoaxostylar granules was 0.9μ. They were structurally indistinguishable from the subcostal granules (Fig. 38).

Paraxostylar granules While the paraxostylar granules were found throughout the organism, they were in greatest concentration in the posterior 2/3 of the organism. They were enclosed by a membrane and had lamellar inclusions (Figs. 36 and 42). The diameter of the paraxostylar granules was a maximum of 1.23μ (Fig. 36). In the anterior 1/3 of the organism (Fig. 36), the lamellar contents of the paraxostylar granules were not as dominant as in the posterior 2/3 (Fig. 42).

Pelta This structure had not been reported from light microscopy studies. The pelta was composed of microtubules of 18mμ diameter (Fig. 43). The kinetosomes of the anterior and recurrent flagella were enclosed within the pelta (Fig. 43). No clear sections of the pelta-axostylar junction were obtained.

Costa The costa was always associated with the base of the undulating membrane (Figs. 38, 42, 44, 46 and 47). In cross-section, the costa was seen to possess a homogeneous matrix (Figs. 35, 42, 44, 45, 46 and 47). A sheath of thin microtubules appeared to surround the costa (Figs. 44, 45, 46 and 47). The diameter of the microtubules of the sheath was 8mμ (Fig. 44). Longitudinal sections of the costa revealed a periodic arrangement of alternate light and dark bands, each with a 28mμ width. The dark band was composed of three dark lines separated by 14mμ (Fig. 38). The costa had a maximum width of 330mμ (Fig. 47).

Subcostal granules These structures were membrane-limited and their contents were homogeneous (Figs. 38 and 47). They were distributed along a line parallel to the costa and on the side opposite the undulating membrane. The maximum diameter of the subcostal granules was 0.9μ (Fig. 47). Structurally, there was no difference between the subcostal granules and the endoaxostylar granules (Figs. 36 and 41).

Undulating membrane This specialized extension of the cytoplasm contained microtubular elements of 16mμ diameter in its outer 1/2 (Fig. 46). These microtubules were arranged in four rows (Figs. 38 and 46). In Fig. 46, they appear to form an inverted "W". The undulating membrane was closely adherent to the recurrent flagellum, separated by a distance of 13mμ (Figs. 36, 37, 38, 42, 44, 46 and 47). There was no distinct connecting element between the recurrent flagellum and the undulating membrane which could be visualized by the techniques used (Fig. 44, arrow).

Anterior flagella The anterior flagella originated in kinetosomes enclosed by the pelta (Fig. 43). The kinetosomes were composed of nine sets of three fibrils each. The fibrils had a diameter of 19mμ and were arranged in a circular pattern with the axes of the sets skewed (Fig. 43). Rootlet structures apparently connected the kinetosomes in the same type of network found in the nasal trichomonads (Fig. 43). The anterior flagella exhibited the normal 9+2 configuration in which the 9 peripheral sets of double fibrils were 16mμ in diameter and the 2 central fibrils were 20mμ in diameter (Fig. 38).

Recurrent flagellum The kinetosome of the recurrent flagellum was oriented at right angles to those of the anterior flagella (Fig. 43). The arrangement of the fibrils in the recurrent flagellum and its kinetosome was identical to that of the anterior flagella and their kinetosomes (Figs. 38, 43, 46 and 47). Longitudinal section of the kinetosome of the recurrent flagellum showed that the peripheral double fibrils of the flagellum continued as the triple fibrils of the kinetosome when they passed below the level of the plasma membrane, but the central single fibrils terminated at this level (Fig. 43, arrow). The recurrent flagellum contained more cytoplasm than did the anterior flagella. The 9+2 arrangement of fibrils occupied the outermost region of the recurrent flagellum (Figs. 42, 44, 46 and 47).

DISCUSSION

On slides made of fixed and stained nasal and stomach trichomonads from the original host, morphological differences were found between the two forms. These included differences in body length and width, nuclear size and parabasal body length. Morphological differences became less pronounced upon prolonged culture.

In my opinion, the original morphological differences between trichomonads from these two sites could be attributed to environmental variations inherent in the two habitats within the host. Differences in pH, temperature, oxygen tension and other conditions are significant when one considers the diverse environments represented by the nasal cavity and the stomach. Kupferberg (1940) and Palmquist and Buttrey (1960) reported morphological changes in trichomonads due to changes of environmental pH. Environmental effects on morphology have been shown to occur in organisms other than protozoa. Watertor (1968) reported the effects of environmental temperature on the morphology of the trematode Telorchis bonnerensis. She determined the optimum temperature for development of the adult trematode to be 30°C. At 34°C, she found the adult worms were of reduced overall size, produced smaller eggs and showed degeneration of reproductive structures. Trematodes reared in hosts maintained at 10°C showed a decreased growth rate and delayed development.

Structural similarities based upon bright field microscopy studies between the nasal and the stomach trichomonads of swine appear to support

the suggestion of Hibler et al. (1960) that they are the same organism, T. suis. In addition, the ultrastructure of the nasal and stomach trichomonads from culture were so similar as to be indistinguishable. For these reasons, they shall be discussed collectively as T. suis.

The ultrastructure of T. suis appears to fit a general trichomonad pattern. The nucleus is the same as that reported from other trichomonads in that it contains nucleolar areas unassociated with membranes, is bound by a double membrane and the entire nucleus is enclosed in rough endoplasmic reticulum. This structural complex is compatible with the general cytological roles played by the nucleus, nucleolus and rough endoplasmic reticulum in that the nucleus contains the genetic information required for cell functions. The enzymes necessary for those functions are synthesized at the ribosomes of the rough endoplasmic reticulum whose RNA (ribonucleic acid) is derived from the nucleolus (Perry, 1960). The proximity of the rough endoplasmic reticulum to the nuclear membrane reflects an efficient organization of cellular components and may indicate a process whereby the rough endoplasmic reticulum is generated directly from nuclear membrane.

The electron micrographs show that the parabasal body is structurally identical to the Golgi apparatus seen in other cells. This is consistent with reports by Anderson and Beams (1961), Simpson and White (1964) and Honigberg, Mattern and Daniel (1968). Functionally, the Golgi apparatus has been linked with synthesis of glycoproteins and mucopolysaccharides (Peterson and LeBlond, 1964 and Neutra and LeBlond, 1965). In addition,

Ostero-Vilardebó et al. (1964) showed sulfation of carbohydrates to occur in the Golgi apparatus. While these studies did not utilize trichomonads as the experimental organism, the general chemical functions of the Golgi apparatus are so consistent that one would expect a similar function in trichomonads. Thus, we would presume the parabasal body to participate in synthesis and/or modification of macromolecular carbohydrates.

The axostylar ultrastructure is essentially identical to that reported for various trichomonads by other investigators. For convenience, I will refer to the cylindrical subunits of the axostyle as microtubules. Whether they are microtubules or microfibrils cannot be determined precisely because of the problems involved with demonstrating whether thay are hollow (Pitelka, 1969). The difference in the arrangement of microtubular subunits of the axostyle found in the anterior and posterior regions of the organism may reflect a difference in functional activity. Anteriorly, the sheet-like arrangement in the capitulum would result in greater flexibility, while overlapping of the axostyle and the pelta in this region would impart stability. Posteriorly, the axostylar shaft has the more rigid form of a closed cylinder. Thus, this one organelle provides varying degrees of flexibility due to variations in arrangement of structural subunits.

During mitosis in trichomonads, it has been reported (Kofoid and Swezy, 1915) that the axostyle splits into two separate axostyles. This is in general agreement with the results obtained for T. suis in which

interlocked double axostyles were sometimes found. Separation of the interlocked axostyles could be interpreted as a splitting of the parental axostyle when viewed by light microscopy. Grimstone (1961) stated that the kinetosomes act as organizers for the synthesis of fibrillar structures in the trichomonads. Mattern, Honigberg and Daniel (1967) considered the paraxostylar granules of T. gallinae to be the source of materials used in the formation and regeneration of the axostyle.

On the basis of the results obtained with T. suis and the reports of Kofoid and Swezy (1915), Grimstone (1961) and Mattern, Honigberg and Daniel (1967), a mechanism for organellogenesis of the axostyle can be formulated. The new axostyle is organized alongside the existing parental axostyle by the kinetosomes, utilizing preformed structural units derived from the paraxostylar granules. The lamellar contents of the paraxostylar granules might well be the workbenches upon which these preformed subunits are synthesized. The presence of the endoaxostylar granules in the capitulum region, and their associated rough endoplasmic reticulum could indicate their involvement in organellogenesis and maintenance of the axostyle.

The costa is also a fibrillar structure originating in the kinetosome region of the karyomastigont complex. Sections in which the costa is found also reveal subcostal granules. These organelles probably participate in functions similar to those of the endoaxostylar granules since they are structurally identical. They could likely serve in organellogenesis of the costa and possibly supply energy for contraction

of the costa. Evidence supporting the energy source concept was published by Sharma and Bourne (1963, 1964 and 1966) in which they reported the presence of Krebs cycle enzymes in the subcostal granules. These granules were found to be PAS-positive by Abraham and Honigberg (1964) and by Sharma and Honigberg (1966), lending additional weight to this concept.

Indeed, a mitochondrial function of this type has been attributed to the subcostal granules and to the paraxostylar granules by Anderson and Beams (1959) and by Hashimoto et al. (1964). Other workers have held that there are no cytoplasmic structures in trichomonads which serve a mitochondrial function (Osada, 1962, Simpson and White, 1964, Nielsen, Ludvik and Nielsen, 1966 and Smith and Stewart, 1966). Mattern, Honigberg and Daniel (1967) considered the subcostal granules to represent an organellogenetic body. Thus, the subcostal, endoaxostylar and paraxostylar granules would provide the macromolecules and energy used in forming new axostyle, pelta and costa with formation of these mastigont structures originating in the kinetosomes (Mattern, Honigberg and Daniel, 1967).

The pelta appears to link the capitulum of the axostyle with the kinetosomes of the anterior and the recurrent flagella. Absence of any mention of a pelta in previous studies of T. suis can be explained as the result of a low affinity of the subunits for stain. Electron microscope studies of various trichomonads have shown peltar structures to exist in T. muris (Anderson and Beams, 1959 and Osada, 1962), T. foetus

(Simpson and White, 1964), T. vaginalis (Nielsen, Ludvik and Nielsen, 1966), T. gallinae (Mattern, Honigberg and Daniel, 1967) and P. hominis (Honigberg, Mattern and Daniel, 1968). In addition, the pelta also serves a morphogenetic function in that its configuration determines the shape of the anterior portion of the trichomonad.

The description of the striated fibrillar nature of the costa of T. suis and its periodicity on the order of 20mμ is in agreement with previously published descriptions of costae of other trichomonads. This periodicity was interpreted as an indication that the costa was composed of collagen (Ohno, 1960 and Perju et al., 1963). However, Simpson and White (1964) were unable to digest the costa with collagenase. It may be more reasonable to interpret the periodic structure of the costa to represent a highly oriented bundle of contractile filaments with the bands corresponding to alignments of repeating subunits of these filaments. The relationship of the costa to the undulating membrane is consistent with all the published reports on trichomonads.

The undulating membrane ultrastructure is in agreement with that found in other trichomonads, but is at variance with results reported for T. gallinae (Mattern, Honigberg and Daniel, 1967) and for P. hominis (Honigberg, Mattern and Daniel, 1968). In both of these species, the undulating membrane was more flattened and extended beyond the recurrent flagellum. This resulted in the recurrent flagellum appearing to be located half-way between the body of the organism and the outer margin of the undulating membrane. These differences might be caused by variations

of technique or could be valid points of morphological difference which could be used as indicators of taxonomic relationships. The trichomonad most similar to T. suis in this respect is T. foetus (Simpson and White, 1964). The cords of microtubular structure seen within the undulating membrane apparently represent the marginal filament of the undulating membrane reported by Buttrey (1956).

The 9+2 arrangement of the anterior and recurrent flagellar fibrils is the same as is seen in all cilia and flagella associated with motility. The network of rootlet fibrils interconnecting the kinetosomes of the anterior and recurrent flagella with the pelta and axostyle is consistent with similar networks seen in the other species of trichomonads. These striated rootlet fibrils may be the means of coordinating the activities of the karyomastigont structures.

The displacement of the fibrils of the recurrent flagellum of T. suis is very similar to that reported by Anderson and Beams (1961) for T. muris and by Simpson and White (1964) for T. foetus. In contrast to these reports, the recurrent flagellum of T. gallinae (Mattern, Honigberg and Daniel, 1967) and of P. hominis (Honigberg, Mattern and Daniel, 1968) had the fibrillar complex located centrally and associated with considerably less cytoplasm than did the flagellum of T. suis.

The structures composing the karyomastigont (nucleus, axostyle, costa, flagella, parabasal body and their accessory structures) are so consistently interrelated that they appear to represent a functional unit. While there is no general agreement on the individual roles each of these structures plays, I propose what I feel is a reasonable hypothetical

model. The central structure of the karyomastigont is the nucleus. It has the information required for synthesis and function of the entire organism. This information is translated by the rough endoplasmic reticulum into enzymes associated with these functions. The parabasal body (Golgi apparatus) acts as a chemical synthesis and/or modification center. Thrust for motility is the function served by the anterior and recurrent flagella. Their activities are controlled by the striated rootlet fibrils which form a network interconnecting the kinetosomes of the flagella.

The thrust produced by the flagella is transmitted to the axostyle-pelta complex which serves primarily a support function. This is similar to the general situation in which force exerted by muscles is transmitted to rigid skeletal structures rather than to softer portions of the metazoa. Contractility of the axostyle is not precluded by a support function. Pitelka (1969) indicated that it is possible for a fibrillar structure to act in both contraction and support.

Directional control of movement appears to be the function of the costa-recurrent flagellum-undulating membrane complex. The costa and the undulating membrane share a common origin and a common terminus. Therefore a shortening of the contractile costa would result in an increased folding of the non-contractile undulating membrane and its recurrent flagellum. This increased folding would automatically result in a greater amplitude and/or frequency of the sine wave configuration of the undulating membrane, thereby producing a change in the vectoral component of the thrust of the undulating membrane and recurrent flagellum. The

undulating membrane is oriented obliquely to the anterior-posterior axis of the organism; therefore, its thrust would affect the direction of the trichomonad's movement.

The height of the undulating membrane also affects its function. I propose that the degree of folding of the fibrils making up the marginal filament controls the height of the undulating membrane. Thus, the anterior flagella provide the primary thrust, while complex interactions of the recurrent flagellum, the undulating membrane with its marginal filament and the costa determine direction of movement. Of course, any axostylar flexion would also have an effect on direction of movement.

Energy required for movement and for synthesis of these structures is provided by the paraxostylar, endoaxostylar and subcostal granules, in addition to their functions in organellogenesis. Although many of these points are speculative, this hypothesis does represent an integrated functional unit consistent with the ultrastructure of T. suis.

Comparison of the ultrastructure of T. foetus (Simpson and White, 1964) with the results obtained for T. suis show great similarity between the two species. These observations, combined with morphological, pathogenic, physiological and serological similarities all support the contention that T. foetus and T. suis should be considered synonymous.

SUMMARY

Cultures of nasal and stomach trichomonads from pigs in the Vermillion, South Dakota, area were grown in cysteine monohydrochloride-peptone-liver infusion-maltose medium (C.P.L.M.). Protargol and iron haematoxylin-stained smears of the trichomonads from the original hosts and from cultures were examined by light microscopy. Initial morphological differences between nasal and stomach trichomonads disappeared upon prolonged culture. Original morphological differences were attributed to environmental differences in the sites of infection.

Specimens for electron microscopy were fixed in phosphate-buffered glutaraldehyde, post-fixed in osmium tetroxide and embedded in epon. Sections were mounted on uncoated grids and were then stained with methanolic uranyl acetate and lead citrate. Electron microscopy showed the organisms from the two cultures to be identical. The nucleus was bounded by a double membrane, included nucleolar areas and was surrounded by concentric layers of rough endoplasmic reticulum. Flattened cisternae of smooth endoplasmic reticulum making up the parabasal body (Golgi apparatus) were associated with small peripheral vesicles. The axostyle was a complex of microtubules in a stockade-like pattern which appeared as a sheet enclosing the karyomastigont structures in the anterior region. Posterior to the nucleus, this microtubular sheet assumed a cylindrical form. Endoaxostylar granules were associated with the anterior region of the axostyle, while paraxostylar granules were associated with both regions.

The pelta was a sheet of microtubules arising internally to the

axostylar capitulum and enclosing the flagellar kinetosomes. Rootlet fibrils interconnected the kinetosomes of the anterior and the recurrent flagella. The striated costa originated at the kinetosome of the recurrent flagellum and terminated at the posterior limit of the undulating membrane. Subcostal granules were described.

The recurrent flagellum was closely associated with the undulating membrane, but no structural connecting element could be resolved. A microtubular complex in the undulating membrane was interpreted as the marginal filament.

Ultrastructural similarities of these two trichomonads and similarities reported by other workers led to the conclusion that they are the same organism, Trichomonas suis . Similarities between T. suis and Trichomonas foetus were seen as indicating these are closely related if not the same species.

A hypothetical mechanism of functional interaction of the mastigont system was proposed in which the axostyle and pelta serve primarily as support elements with thrust for motility arising from movements of the anterior and recurrent flagella. Contraction of the costa was hypothesized as an additional source of thrust as well as the source of the vectoral component of movement by changing the amplitude of the undulating membrane sine wave. Kinetosomal rootlet fibrils were assigned a communication and coordination function.

LITERATURE CITED

Abraham, R. and Honigberg, B. M. 1964. Structure of Trichomonas gallinae (Rivolta). J. Parasit. 50: 608-619.

Anderson, E. 1955. The electron microscopy of Trichomonas muris. J. Protozool. 2: 114-124.

Anderson, E. and Beams, H. W. 1959. The cytology of Tritrichomonas as revealed by the electron microscope. J. Morphol. 104: 205-235.

Anderson, E. and Beams, H. W. 1961. The ultrastructure of Tritrichomonas with special reference to the blepharoplast complex. J. Protozool. 8: 71-75.

Brumpt, E. J. A. 1936. Précis de parasitologie. Vol. 1. 5th ed. Paris, France, Masson et Cie.

Buttrey, B. W. 1956. A morphological description of a Tritrichomonas from the nasal cavity of swine. J. Protozool. 3: 9-13.

Chakraborty, J., Das Gupta, N. N. and Ray, H. N. 1961. An electron microscope study of the Trichomonas criceti. Cytologia 26: 320-326.

Davaine, C. J. 1877. Traité des entozoaires et des maladies vermineuses de l'homme et des animaux domestiques. 2nd ed. Paris, France, Bailliere et fils. Original not available; cited by Hibler, D. P., Hammond, D. M., Caskey, F. H., Johnson, A. E. and Fitzgerald, P. R. 1960. The morphology and incidence of the trichomonads of swine, Tritrichomonas suis (Gruby and Delafond), Tritrichomonas rotunda, n. sp. and Trichomonas buttreyi, n. sp. J. Protozool. 7: 159-171.

Doran, D. J. 1957. Studies on trichomonads. I. The metabolism of Tritrichomonas foetus and trichomonads from the nasal cavity and cecum of swine. J. Protozool. 4: 182-190.

Doran, D. J. 1959. Studies on trichomonads. III. Inhibitors, acid production and substrate utilization by 4 strains of Tritrichomonas foetus. J. Protozool. 6: 177-182.

Fitzgerald, P. R., Johnson, A. E., Thorne, J. L. and Hammond, D. M. 1958. Experimental infections of bovine genital system with trichomonads from the digestive tracts of swine. Am. J. Vet. Res. 19: 775-779.

Frye, W. W. and Meleney, H. E. 1932. Investigations of Endamoeba histolytica and other intestinal protozoa in Tennessee: IV. A study of flies, rats, mice and some domestic animals as possible carriers of intestinal protozoa of man in a rural community. Am. J. Hyg. 16: 729-749.

Grimstone, A. V. 1961. Fine structure and morphogenesis in Protozoa. Biol. Rev. 36: 97-150.

Gruby, D. and Delafond, H. M. O. 1843. Recherches sur des animalcules se développant en grande nombre dans l'estomac et dans les intestins, pendant la digestion des naimaux herbivores et carnivores. Compt. Rend. Acad. Sci. 17: 1304-1308.

Hammond, D. M. and Leidl, W. 1957. Experimental infections of the genital tract of swine and goats with Trichomonas foetus and Trichomonas species from the cecum or feces of swine. Am. J. Vet. Res. 18: 461-465.

Hammond, D. M., Fitzgerald, P. R. and Johnson, A. E. 1957. Incidence of trichomonads in the digestive tract and nose of pigs in the western United States. J. Parasit. 43: 695-696.

Hashimoto, M., Komori, A., Kuramasu, T., Yokoyama, Y., Kawase, N. and Nakamura, T. 1964. Electron microscope studies on the fine structure of Trichomonas vaginalis. J. Jap. Obstet. Gynec. Soc. 11: 162-166.

Hibler, C. P., Hammond, D. M., Caskey, F. H., Johnson, A. E. and Fitzgerald, P. R. 1960. The morphology and incidence of the trichomonads of swine, Tritrichomonas suis (Gruby and Delafond), Tritrichomonas rotunda, n. sp. and Trichomonas buttreyi, n. sp. J. Protozool. 7: 159-171.

Honigberg, B. M., Mattern, D. F. T. and Daniel, W. A. 1968. Structure of Pentatrichomonas hominis (Davaine) as revealed by electron microscopy. J. Protozool. 15: 419-430.

Inoki, S., Nakanishi, K. and Nakabayashi, T. 1959. Observations on Trichomonas vaginalis by electron microscopy. Biken's J. 2: 21-24.

Inoki, S., Nakanishi, K. and Nakabayashi, T. 1960. Electron microscopic observations of Trichomonas vaginalis employing the thin-section technique. Gynaecologia 149: 48-54.

Inoki, S., Ohno, M., Kondo, K. and Sakamoto, H. 1961. Electron-microscopic observations of the 'costa' as one of the organelles in Trichomonas foetus. Biken's J. 4: 63-65.

Johnson, G. J. 1947. The physiology of bacteria-free Trichomonas vaginalis. J. Parasit. 33: 189-198.

Kerr, W. R. 1958. Experiments in cattle with Trichomonas suis. Vet. Rec. 60: 613-615.

Kessel, J. F. 1928a. Intestinal protozoa of the domestic pig. Am. J. Trop. Med. 8: 481-501.

Kessel, J. F. 1928b. Trichomoniasis in kittens. Royal Soc. Trop. Med. and Hyg., Trans. 22: 61-80.

Kofoid, C. A. and Swezy, O. 1915. Mitosis and multiple fission in trichomonad flagellates. Am. Acad. Arts and Sci., Proc. 51: 287-379.

Kupferberg, A. B. 1940. Physiology of pure cultures of Trichomonas vaginalis. II. Cell size in relation to pH. Soc. Exp. Biol. Med., Proc. 45: 220-221.

Künstler, J. 1888. Sur quelques infusories nouveaux ou peu connus. Compt. Rend. Acad. Sci. 107: 953-955.

Küst, D. 1936. Die Diagnose der Trichomonadenseuche des Rindes. Deutsche Tierärztl. Woch. 44: 821-825.

Mattern, C. F. T., Honigberg, B. M. and Daniel, W. A. 1967. The mastigont system of Trichomonas gallinae (Rivolta) as revealed by electron microscopy. J. Protozool. 14: 320-339.

McNutt, S. H., Blohm, F. and Barger, J. A. 1939. Incidence of Trichomonas foetus infection in Iowa. Vet. Med. 34: 40-42.

Neutra, M. and LeBlond, C. P. 1965. Synthesizing complex carbohydrates in the Golgi regions as shown by the uptake of tritiated galactose. J. Cell Biol. 27: 72A.

Nie, D. 1950. Morphology and taxonomy of the intestinal protozoa of the guinea pig, Cavia porcella. J. Morph. 86: 381-494.

Nielsen, M. H. and Ludvik, J. 1964. On the ultrastructure of Trichomonas vaginalis. Europ. Reg. Cong. Electron Micr., Proc., Czech. Acad. Sci., Prague, 3: 181-182.

Nielsen, M. H., Ludvik, J. and Nielsen, R. 1966. On the ultrastructure of Trichomonas vaginalis Donné. J. Micros. 5: 299-350.

Ohno, M. 1960. Studies on the fine structures of Trichomonas tenax by means of electron microscopy. Osaka Univ. Med. J. 12: 563-569.

Osada, M. 1962. Electron microscopic studies of protozoa (Trichomonas muris). Keio J. Med. 11: 227-252.

Ostero-Vilardebó, L. R., Lane, N. and Godman, G. C. 1964. Some characteristics of cells secreting sulfated mucopolysaccharides. J. Histochem. Cytochem. 12: 34.

Palmquist, D. and Buttrey, B. W. 1960. The relation of hydrogen-ion concentration to growth and size of a porcine trichomonad from the caecum. South Dakota Acad. Sci., Proc. 39: 109-116.

Perju, A., Pertrea, E. and Toader, V. 1963. Étude au microscope électronique de l'action de 1 (hydroxy-2'éthyl)-1 méthyl-2 nitro-5 imidazole sur l'infrastructure de Trichomonas vaginalis. Gyn. Prat. 14: 199-215.

Perry, R. P. 1960. On the nucleolar and nuclear dependence of cytoplasmic RNA synthesis in HeLa cells. Exp. Cell Res. 10: 216-220.

Peterson, M. R. and LeBlond, C. P. 1964. Uptake by the Golgi region of glucose labelled with tritium in the 1 or 6 position as an indicator of synthesis of complex carbohydrate. Exp. Cell Res. 34: 420-423.

Pitelka, D. R. 1969. Fibrillar systems in Protozoa. In Chen, T. Research in Protozoology. Vol. 3. Pp. 279-388. New York, New York, Pergamon Press, Inc.

Randall, L. A. 1960. Comparative morphology of the trichomonad flagellates from the nasal cavity, stomach and caecum of swine. Unpublished M.S. thesis. Vermillion, South Dakota, Library, State University of South Dakota.

Randall, L. A. and Buttrey, B. W. 1961. Comparative morphology of the trichomonad flagellates from the nasal cavity, stomach and caecum of swine. South Dakota Acad. Sci., Proc. 40: 52-58.

Sanborn, W. R. 1955. Microagglutination reactions of Trichomonas suis, T. sp. and T. foetus. J. Parasit. 41: 295-298.

Sharma, N. N. and Bourne, G. H. 1963. Studies on the histochemical distribution of oxidative enzymes in Trichomonas vaginalis. J. Histochem. and Cytochem. 11: 628-634.

Sharma, N. N. and Bourne, G. H. 1964. Studies on the histochemical distribution of hydrolases in Trichomonas vaginalis. Acta Histochem. 18: 213-221.

Sharma, N. N. and Bourne, G. H. 1966. Histochemical demonstration of some DPN and TPN-linked dehydrogenases in Trichomonas vaginalis. Acta Histochem. 23: 23-30.

Sharma, N. N. and Honigberg, B. M. 1966. Cytochemical observations on chick liver cell cultures infected with Trichomonas vaginalis. I. Nucleic acids, polysaccharides, lipids and proteins. J. Parasit. 52: 538-555.

Shaw, R. F. and Buttrey, B. W. 1958. Inoculations of Tritrichomonas sp. from the nasal cavity of swine into parasite-free chickens. South Dakota Acad. Sci., Proc. 37: 35-37.

Simpson, C. F. and White, F. H. 1964. Structure of Trichomonas foetus as revealed by electron microscopy. Am. J. Vet. Res. 25: 815-824.

Smith, B. F. and Stewart, B. T. 1966. Fine structure of Trichomonas vaginalis. Exp. Parasit. 19: 52-63.

Switzer, W. P. 1951a. Incidence, cultivation, morphology and certain host relationships of a Trichomonas sp. (Protozoa: Zoomastigina) occurring in the nasal cavity of swine. Unpublished M.S. thesis. Ames, Iowa, Library, Iowa State University of Science and Technology.

Switzer, W. P. 1951b. Atrophic rhinitis and trichomonads. Vet. Med. 46: 478-481.

Trussell, R. E. 1947. Trichomonas vaginalis and trichomoniasis. Springfield, Illinois. Charles C. Thomas Co.

Venable, J. H. and Coggeshall, R. 1965. A simplified lead citrate stain for use in electron microscopy. J. Cell Biol. 25: 407-408.

Watertor, J. L. 1968. Effects of temperature stress on growth and development of larval and adult Telorchis bonnerensis (Trematoda: Telorchiidae). J. Parasit. 54: 506-508.

Yeh, Y., Huang, M. T. and Lien, W. N. 1966. Fine structure of Trichomonas vaginalis with special reference to the mastigont system and the structure of mitochondria. Chinese Med. J. 85: 375-390. Original not available; cited by Mattern, C. F. T., Honigberg, B. M. and Daniel, W. A. 1967. The mastigont system of Trichomonas gallinae (Rivolta) as revealed by electron microscopy. J. Protozool. 14: 320-339.

FIGURES

Figs. 1 - 34: Nasal trichomonad

Fig. 1. Nucleolar areas (Nc) are found in the nucleus (N) which is surrounded by rough endoplasmic reticulum (ER). The costa (C) is sectioned near its origin at the kinetosome of the recurrent flagellum (R). Also seen in this figure are paracostal granules (PG). X23,000.

Fig. 2. Spatial relationships of the axostyle (Ax), nucleus (N) and parabasal body (PB) are shown in this figure. Note the lamellae comprising the parabasal body. Paraxostylar granules (PG) are associated with the axostyle. The costa (C) has a consistent position with respect to the undulating membrane (U) and its recurrent flagellum (R). Subcostal granules (SG) lie below the costa. X17,200.

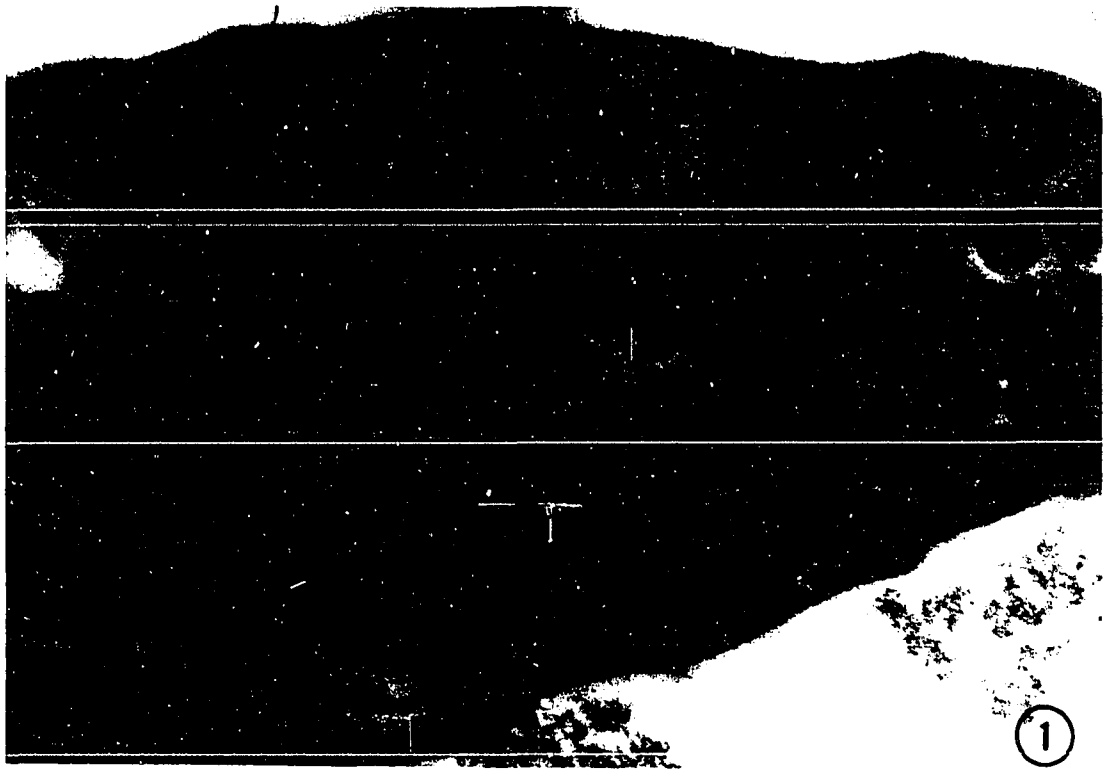
1

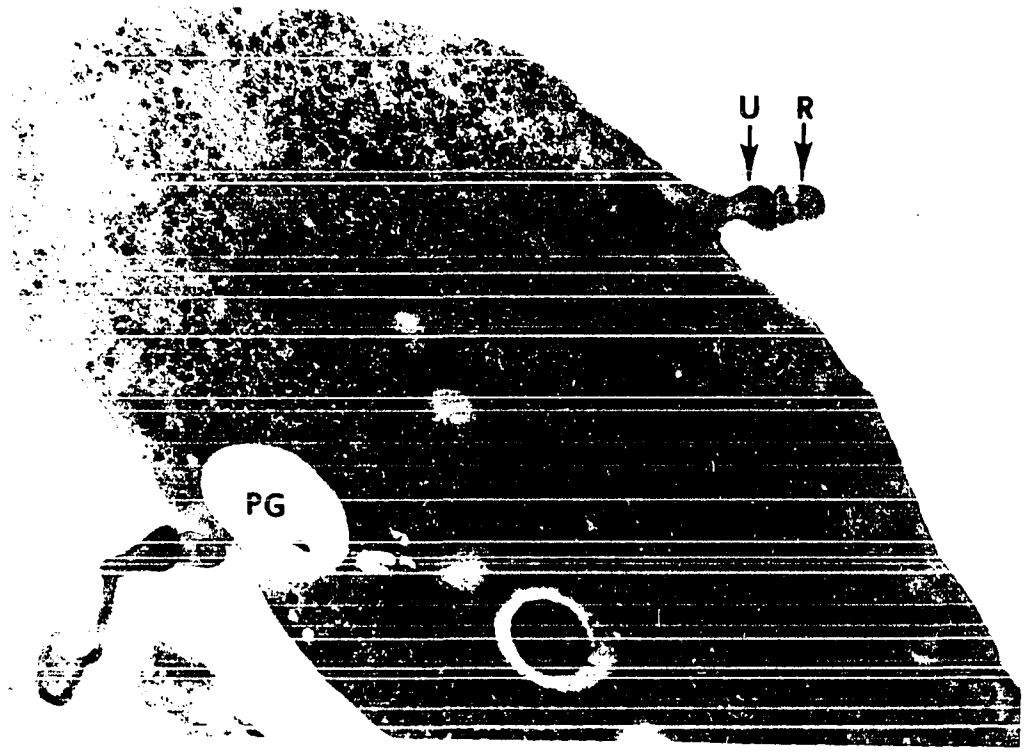
U
R
PG

Fig. 3. The presence of nucleolar areas (Nc) in the nucleus (N) are seen here. Note the double membrane surrounding the nucleus. Two sections of the flexed costa (C) appear with subcostal granules (SG) nearby. Endoaxostylar granules (EG) found in the axostyle (Ax) appear very similar in structure to subcostal granules. The recurrent flagellum (R) has no visible elements connecting it with the undulating membrane (U). X25,800.

Fig. 4. Association of the endoaxostylar granule (EG) with one end of the sheet-like axostylar capitulum (Ax) is shown, with a paraxostylar granule (PG) nearby. Also in this section, the relationships of nucleus (N) to rough endoplasmic reticulum (ER) and those of the costa (C), undulating membrane (U) and recurrent flagellum (R) are seen. Note the large amount of cytoplasm in the recurrent flagellum and the displacement of the fibrils away from the undulating membrane. X30,200.

Fig. 5. The open axostylar capitulum (Ax) containing endoaxostylar granules (EG) faces the nucleus (N) which contains a nucleolar area (Nc). Near the axostyle is a paraxostylar granule (PG). The costa (C) is near the undulating membrane (U) with its recurrent flagellum (R). X19,800.

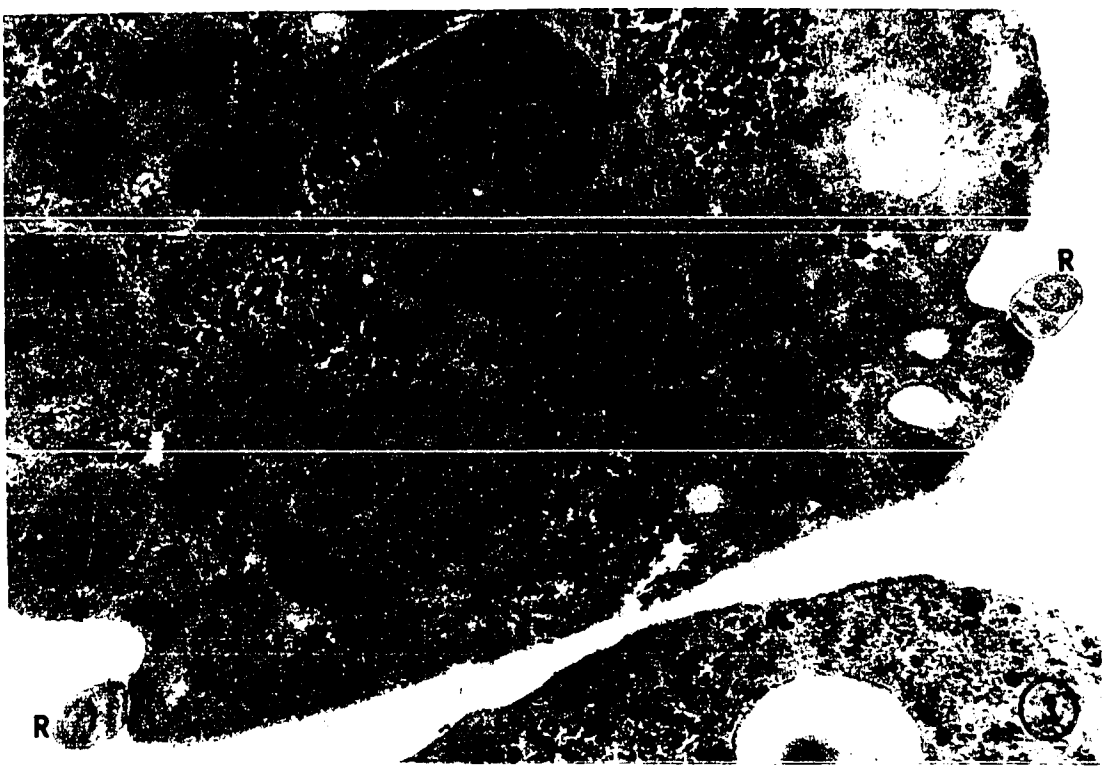
R
R

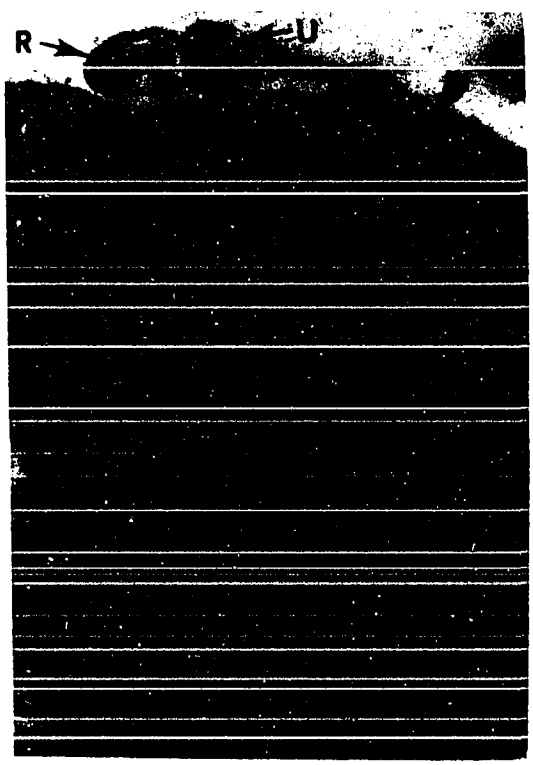
R
U


U
R
5

Fig. 6. The axostylar capitulum (Ax) encloses the parabasal body (PB) which is composed of flattened cisternae of smooth endoplasmic reticulum with numerous small vesicles along the periphery. Terminal portions of the pelta (Pe) and a section of the costa (C) also appear. X27,900.

Fig. 7. A longitudinal section of the parabasal body (PB) shows the same structure as the cross section in Fig. 6. Periodicity of the costa (C) is evident in longitudinal section. The membrane-limited endoaxostylar granule (EG) is located between the parabasal body and the axostyle. X27,600.

Fig. 8. This figure shows the parabasal body (PB) located within the axostylar capitulum (Ax). The costa (C) is just beneath the undulating membrane (U) and its associated recurrent flagellum (R). X26,000.

Fig. 9. The parabasal body (PB) lies alongside the nucleus (N) which has been cut tangentially. X26,000.

Fig. 10. The terminal portion of a flagellum (arrow a) has nine peripheral single tubules and two central single tubules, while a more proximal section shows nine peripheral double tubules with two central single tubules. X30,900.

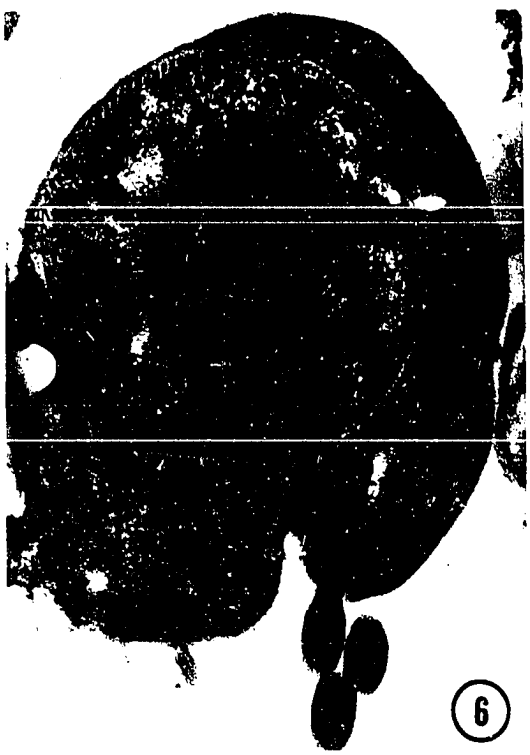
6


7


R
U
C
PB
Ax
8

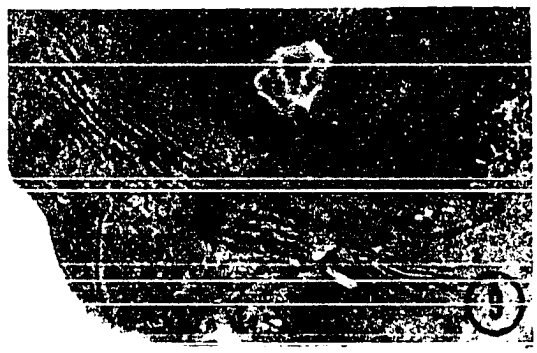
9

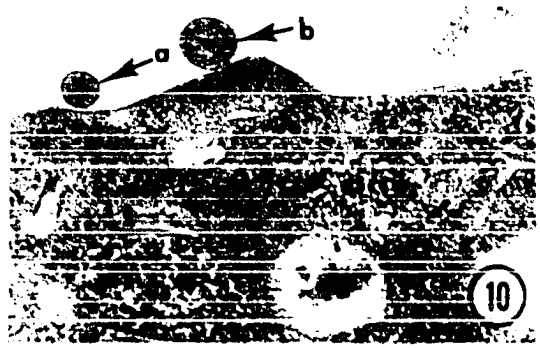
a
b
10

Fig. 11. A cross-section in the posterior region of the trichomonad shows the cylindrical axostyle (Ax) composed of microtubules. Alongside the axostyle is a paraxostylar granule (PG) with a tangential section of its lamellar contents. The recurrent flagellum (R) has become independent of the body of the organism at this level. X28,200.

Fig. 12. The axostyle (Ax) forms a juncture with the pelta (Pe) which encloses the kinetosomes of the anterior flagella (1, 2 and 3). The costa (C) originates in this area at the kinetosome of the recurrent flagellum (not in this section). Located within the curvature of the axostylar capitulum are endoaxostylar granules (EG). The nucleus (N) is surrounded by rough endoplasmic reticulum (ER). X22,200.

Fig. 13. The nucleus (N) and its rough endoplasmic reticulum (ER) along with an endoaxostylar granule (EG) lie inside the axostylar capitulum (Ax). The pelta (Pe) originates inside the axostyle at the pelta-axostylar junction (arrow). The kinetosomes of the anterior flagella are oriented with no. 1 dorsally (1), no. 2 medially (2) and no. 3 ventrally (3). Perpendicular to these is the kinetosome of the recurrent flagellum (R). This section also shows rootlet filaments of the kinetosomes of the anterior flagella no. 2 and no. 3 (F_2 and F_3 respectively). X41,700.


12

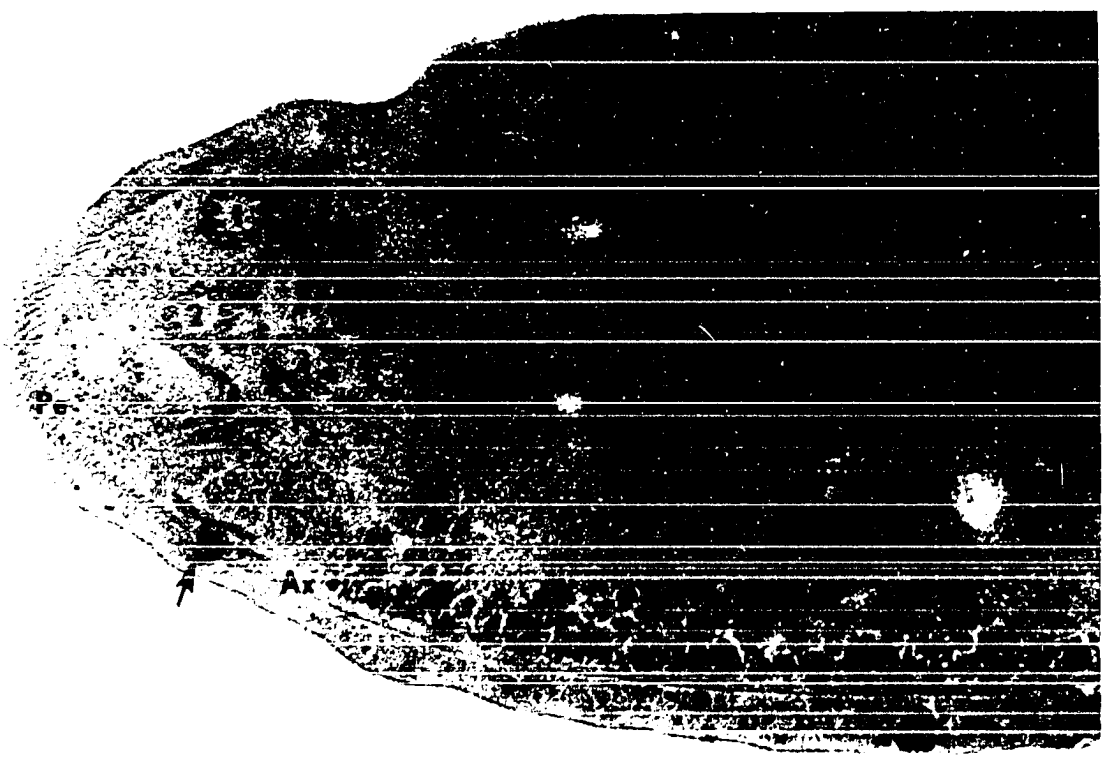
Fe
Ax

Fig. 14. At one edge of the axostylar capitulum (Ax) is an endoaxostylar granule (EG). Associated with this area are the parabasal body (PB) and the pelta (Pe). The undulating membrane (U) is a cytoplasmic modification with the costa (C) below it and the recurrent flagellum (R) along its outer margin. X23,600.

Fig. 15. The axostyle (Ax), when sectioned below the level of the nucleus appears as a nearly closed cylinder. The endoaxostylar granule (EG) is associated with one edge of the axostylar sheet. Lamellar contents of the paraxostylar granule (PG) are prominent. The costa (C) also appears in this section. X20,000.

Fig. 16. In this oblique section, the axostylar capitulum (Ax) and its associated pelta (Pe) enclose most of the structures in the anterior portion of the trichomonad. Included in these structures are the parabasal body (PB), endoaxostylar granules (EG), costa (C) and kinetosomes (1 and 2). At the junction of the axostyle and pelta, the pelta is seen to lie inside the axostyle. X30,400.


U
R
14

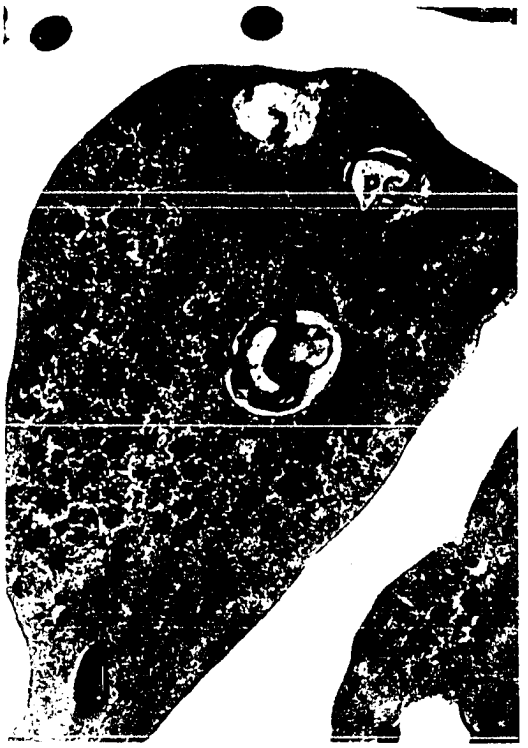
PC


AI
16

Fig. 17. The nearly closed axostyle (Ax) has an endoaxostylar granule (EG) associated with one edge of the sheet of microtubules. A paraxostylar granule (PG) is located nearby. X28,100.

Fig. 18. Two axostyles are present in this organism which was preparing for mitosis. The axostyles (Ax) are interlocked. X38,000.

Fig. 19. The kinetosomes of the anterior flagella (1, 2 and 3) have rootlet filaments (F_1, F_2 and F_3). They are enclosed by the pelta (Pe) which forms a junction with rootlet filament no. 2 (F_2) and the axostyle (Ax). X41,200.

Fig. 20. The axostyle (Ax) is surrounded by paraxostylar granules (PG). Rough endoplasmic reticulum (ER) surrounds the endoaxostylar granules (EG) in the anterior region. Nearby is the lamellate parabasal body (PB). The costa (C) lying under the undulating membrane (U) with its recurrent flagellum (R) is also accompanied by subcostal granules (SG). Also in this view are two anterior flagella (AF) in longitudinal section. X23,600.

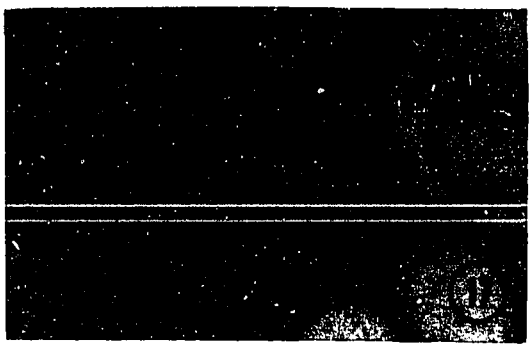

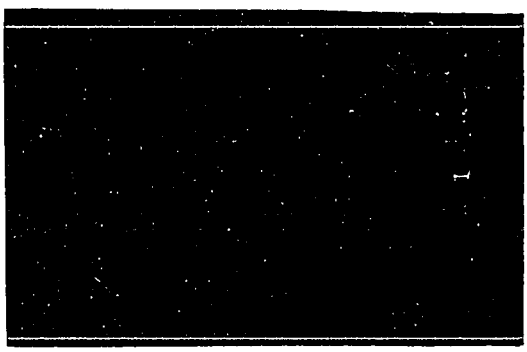

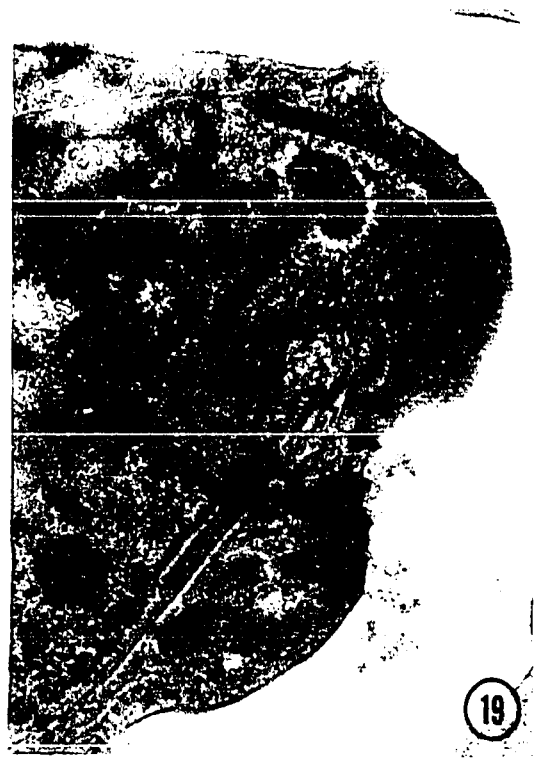
19

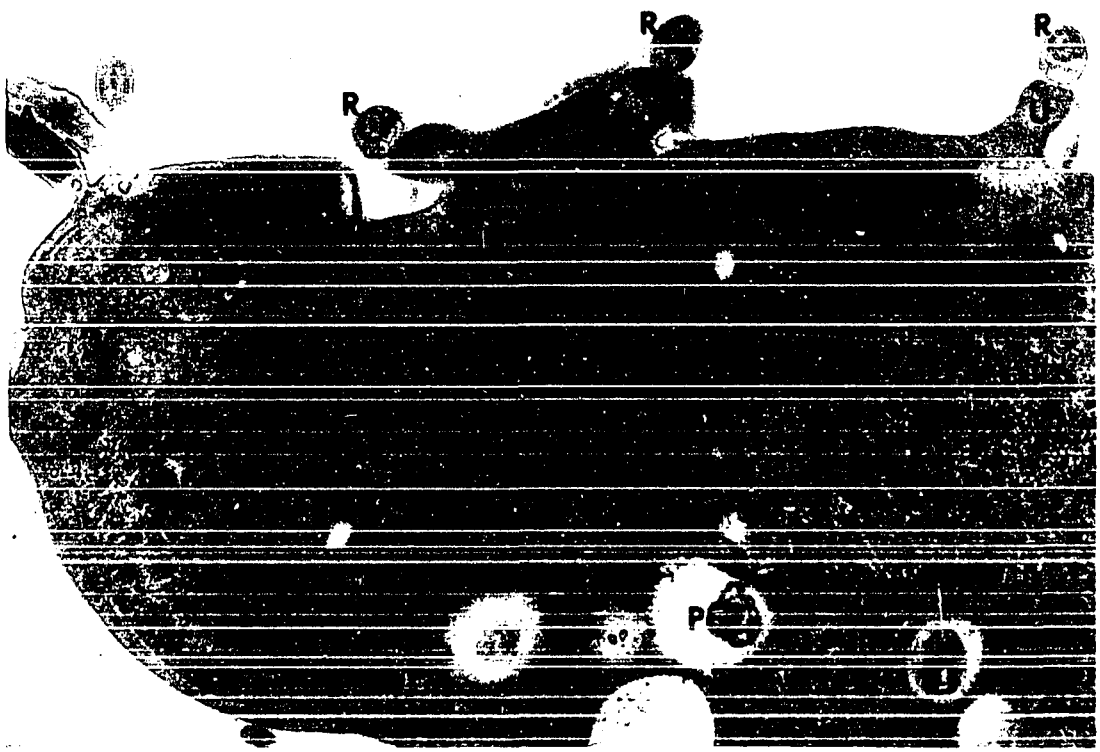
R
R
R
P

Fig. 21. The curvature of the fibrils of the pelta (Pe) over the kinetosomes (1, 2 and 3) determines the form of the anterior portion of the trichomonad. The costa (C) originates in this region in the area of the kinetosome of the recurrent flagellum (not seen in this section). The undulating membrane (U) and the recurrent flagellum (R) appear closely associated but no attachment is visible. X27,200.

Fig. 22. The junction between the axostyle (Ax) and pelta (Pe) shows the pelta to be internal to the axostyle. There is a striated rootlet fibril (F) connecting the kinetosome of the recurrent flagellum (R) to the pelta. The costa (C) appears to originate at the kinetosome of the recurrent flagellum. X19,000.

Fig. 23. Origin of the costa (C) at the kinetosome of the recurrent flagellum (R) and the undulating membrane's relationship to the recurrent flagellum are shown. The tubular elements of the recurrent flagellum occupy the outer region of the flagellum. X35,300.


R
U
1
2
P
21


Pe
F
R
22

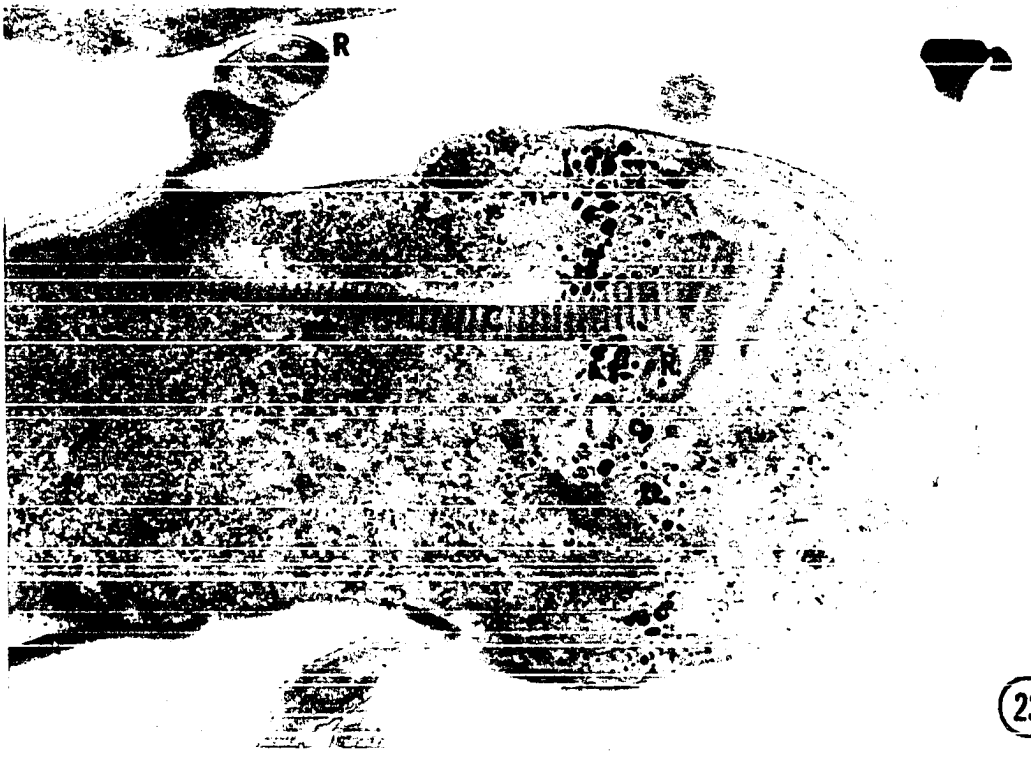
R
23

Fig. 24. Anterior flagella arise from the periflagellar pit (PF), an indentation of the anterior portion of the organism. The skewed arrangement of the nine triplet microtubules of the kinetosome of the recurrent flagellum (R) have an electron-dense region in the center. Below the kinetosome is the costa (C) which originates at the kinetosome of the recurrent flagellum. The parabasal body (PB) is also present in this section. X51,300.

Figs. 25-28. Views of the undulating membrane (U), recurrent flagellum (R), costa (C) and pericostal sheath (S). The distinct space between the undulating membrane and recurrent flagellum is prominent in Figs. 25 and 28. The pericostal sheath (S) seen in longitudinal section (Figs. 25 and 26) and in cross section (Figs. 27 and 28) indicate the sheath completely encloses the costa.

Fig. 25. X46,900.

Fig. 26. X31,900.

Fig. 27. X41,400.

Fig. 28. X32,300.

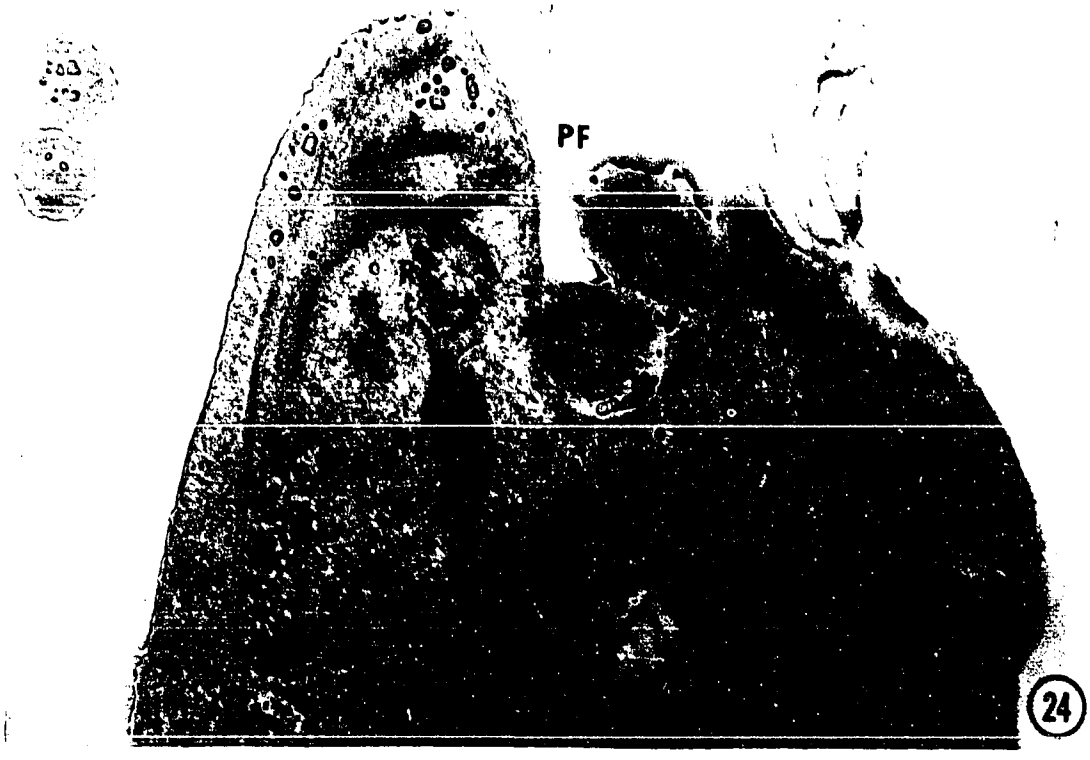
PF
24

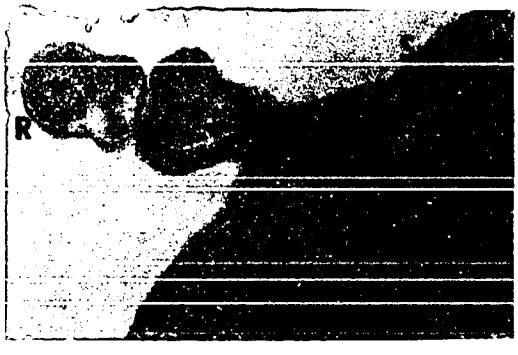
R

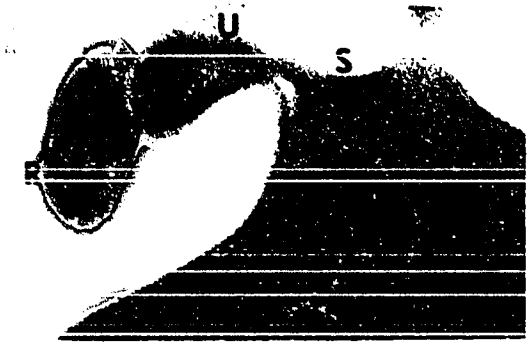
U
S

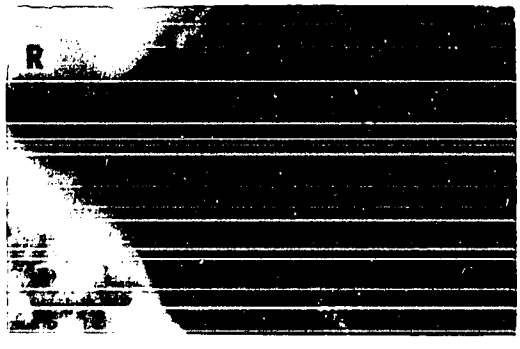
R

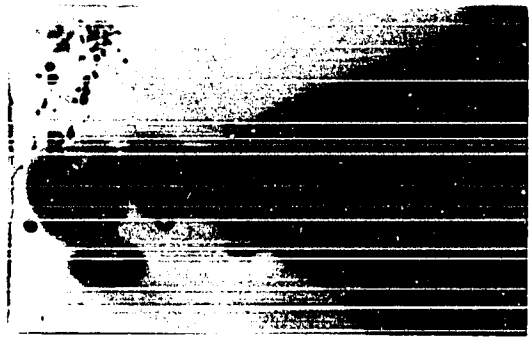

Fig. 29. Below the costa (C) are subcostal granules (SG). There are rows of microtubules in the undulating membrane (U) near the recurrent flagellum (R). X32,000.

Fig. 30. The 9+2 arrangement of fibrils in the recurrent flagellum (R) is very prominent in the outer region of the flagellum. There are four rows of microtubules (arrows) in the undulating membrane (U). X40,000.

Fig. 31. Subcostal granules (SG) parallel the costa (C) on the side opposite the undulating membrane (U) and recurrent flagellum (R). The subcostal granule is membrane-limited. X43,400.

Fig. 32. Posterior to the nucleus, the axostyle (Ax) appears to be cylindrical, and has been cut obliquely in this section. There is a paraxostylar granule (PG) nearby. The nucleus (N) contains a nucleolar area (Nc). The undulating membrane (U) contains rows of microtubular or vesicular elements (arrows). Other structures in this figure are the costa (C) and the recurrent flagellum (R). X24,400.

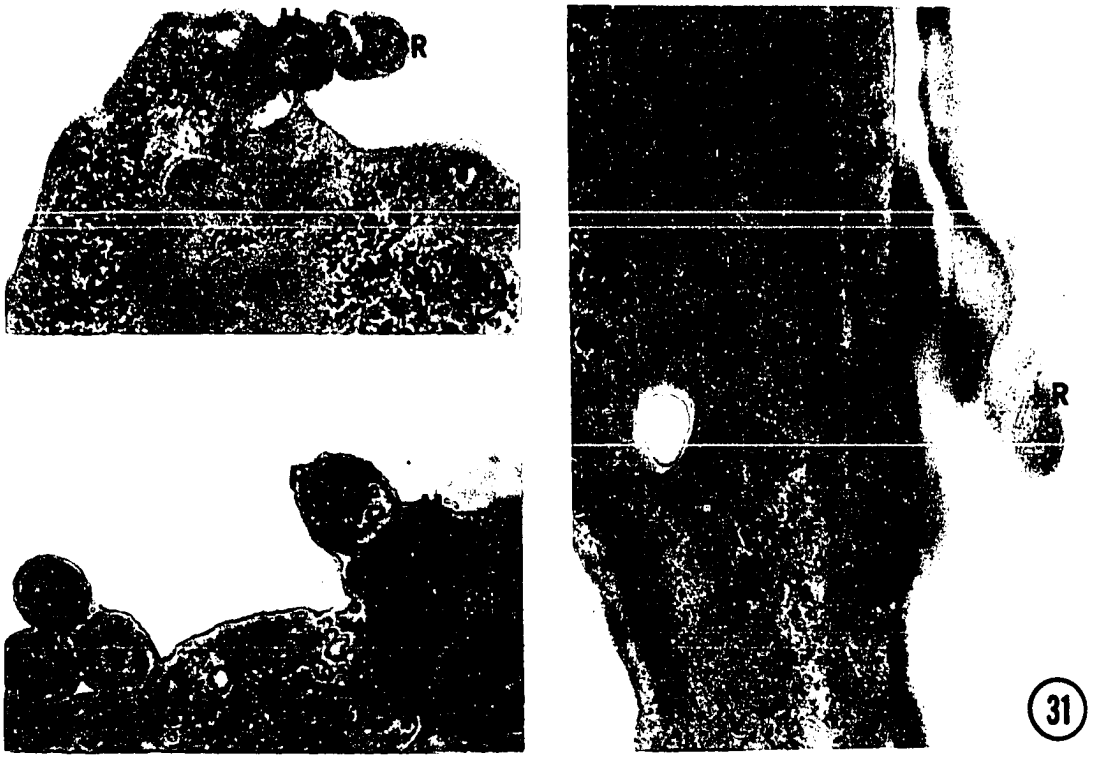
R
R
31


R
R
U
U
31

Fig. 33. Rootlet filaments (F) of the kinetosomes (K) of anterior flagella appear to connect the kinetosomes to each other and to the pelta (Pe). Note the skewed set of nine triplet fibrils in the kinetosomes and the dense central areas. X43,100.

Fig. 34. In the terminal portion of a flagellum, the sets of nine peripheral double fibrils is reduced to a set of nine single fibrils (arrow). The central fibrils persist. X43,100.

Figs. 35 - 47: Stomach trichomonad

Fig. 35. Nucleolar areas (Nc) are found in the nucleus (N) which is bounded by a double membrane and enclosed in rough endoplasmic reticulum (ER). Nearby is the costa (C). X24,800.

Fig. 36. The axostylar capitulum (Ax) encloses the nucleus (N), parabasal body (PB) and endoaxostylar granules (EG). The paraxostylar granules (PG) are found outside the capitulum. Flattened cisternal elements, swollen along the periphery and associated with small vesicles make up the parabasal body. X16,300.

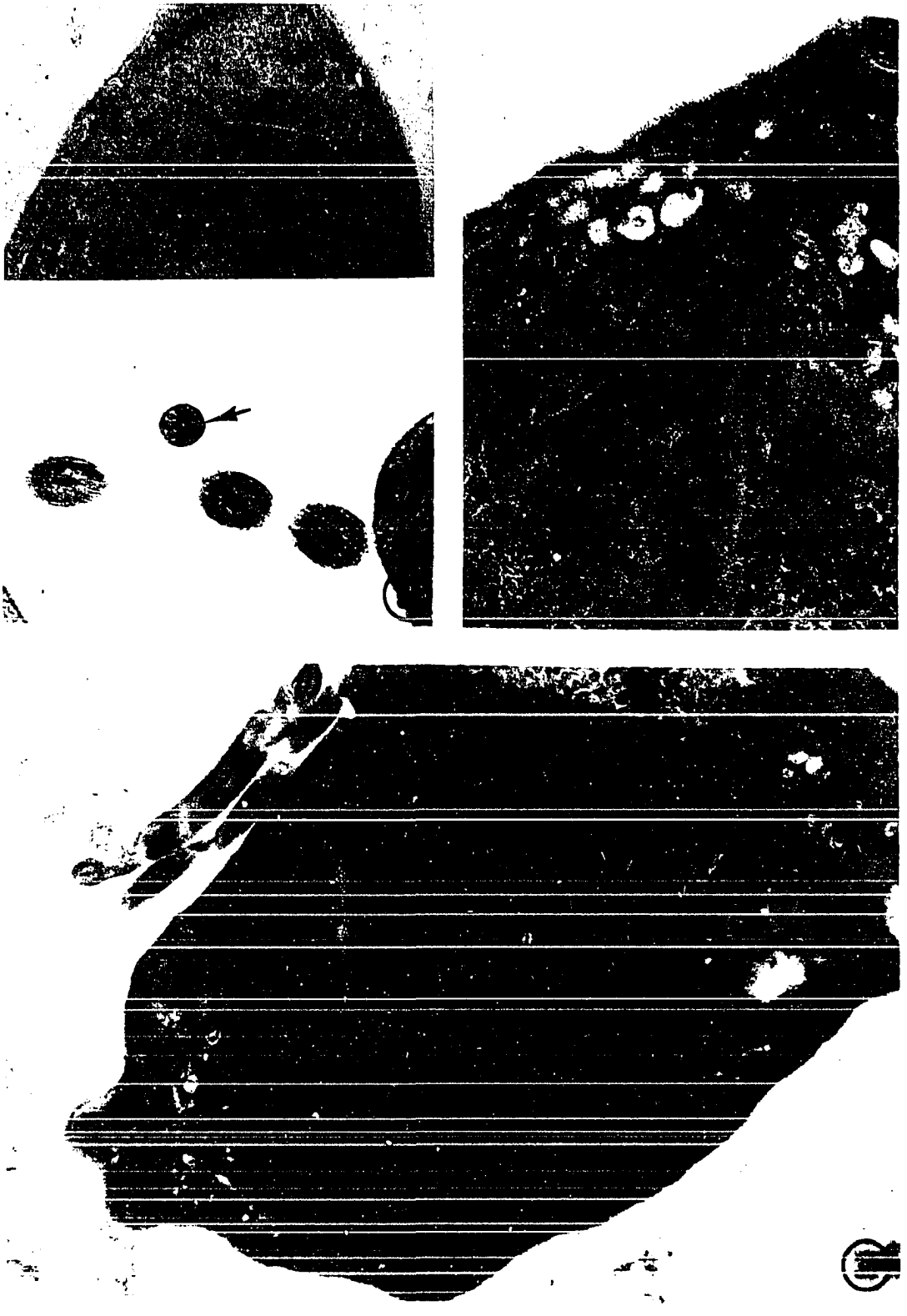

Fig. 37. The nucleus (N) contains nucleolar areas (Nc) and lies inside the capitulum of the axostyle (Ax). The undulating membrane (U) is associated with the recurrent flagellum (R) but no definite connecting structure can be resolved. X13,300.

Fig. 38. Beneath the undulating membrane (U) is the costa (C) with subcostal granules (SG) below it. The undulating membrane appears to contain four rows of microtubules. Other structures present in this section are the anterior flagella (AF), recurrent flagellum (R) and parabasal body (PB). X25,000.

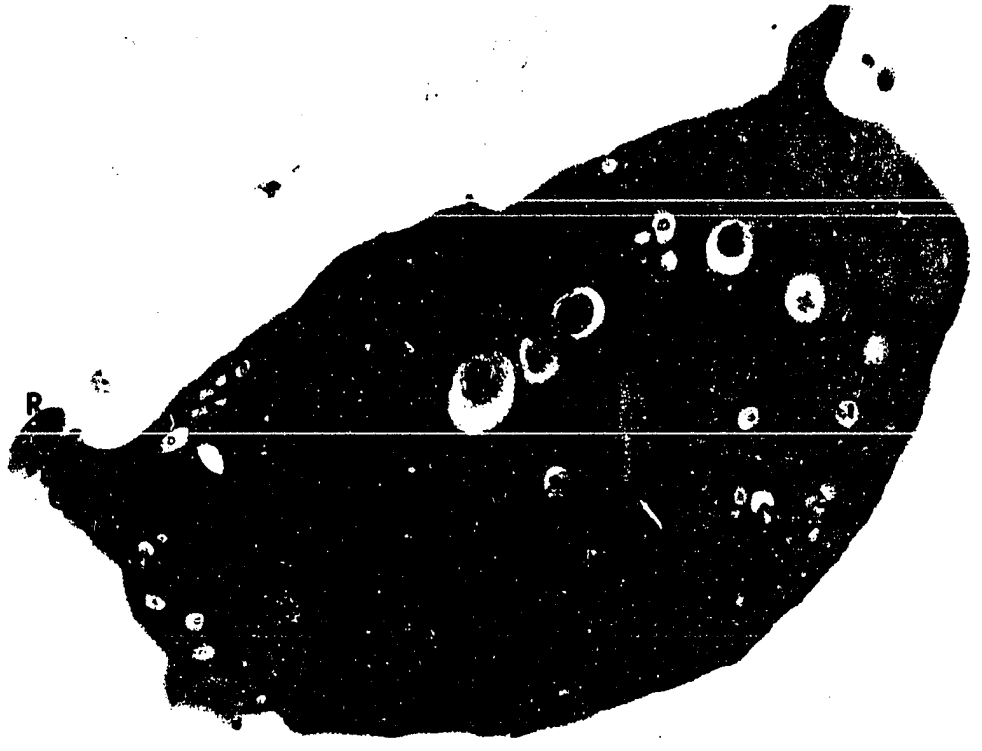

(37)

Figs. 39 and 40. Posterior cross sections of the axostyle (Ax) reveal a circular configuration of microtubular elements containing granular material.

Fig. 39. X50,000.

Fig. 40. X34,500.

Fig. 41. The axostylar capitulum (Ax) encloses endoaxostylar granules (EG) which are limited by a single thickness of membrane and have a homogeneous matrix. X27,300.

Fig. 42. This organism possesses two axostyles (Ax) which are interlocked but not completely closed. This is an initial step in reproduction of the trichomonad. Nearby is a group of paraxostylar granules (PG). The costa (C), undulating membrane (U) and recurrent flagellum (R) are also present. X23,100.

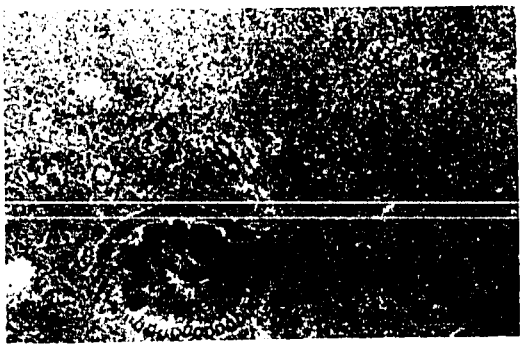

40

41

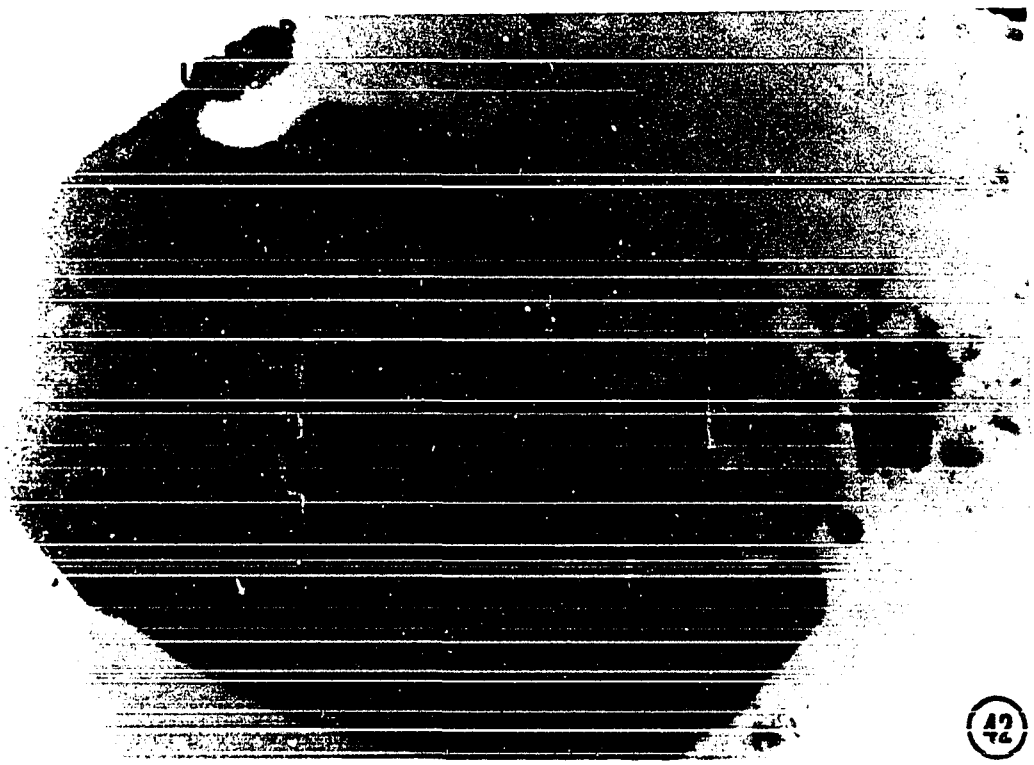

42

Fig. 43. In the anterior region, the pelta (Pe) encloses the kinetosomes of the anterior (1, 2 and 3) and recurrent flagella (R). Kinetosome no. 2 has a rootlet fibril (F_2) attached. Peripheral double fibrils of the recurrent flagellum continue into the cytoplasm as the triplet fibrils of the kinetosome, but the central pair of single tubules terminate at the level of emergence of the flagellum from the body of the trichomonad (arrow). X36,200.

Fig. 44. A space between the recurrent flagellum (R) and the undulating membrane (U) is evident in this longitudinal section. Also present is the costa (C) with its pericostal sheath (S). X37,600.

Fig. 45. At high magnification, the detail of the pericostal sheath (S) around the costa (C) appears as a series of very fine microtubular elements. X45,300.

Fig. 46. The 9+2 arrangement of fibrils in the recurrent flagellum (R) occupies the outermost portion of the flagellum. Inside the undulating membrane (U) is a set of microtubules arranged in four rows as an inverted W-shaped complex. Also present are the costa (C) and the pericostal sheath (S). X42,000.

Fig. 47. This section shows the undulating membrane (U) and recurrent flagellum (R) overlapping the anterior flagella (AF). Microtubular elements are seen in both longitudinal and transverse sections of the undulating membrane. The costa (C), pericostal sheath (S) and subcostal granules (SC) are also present. X24,300.


43


R
U
S

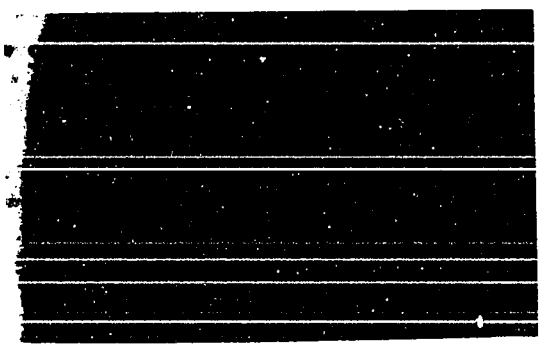

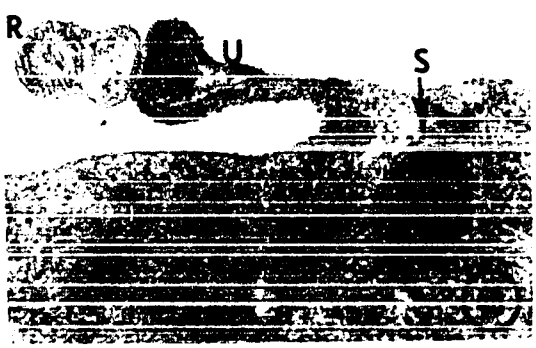
R
U
S


R
U

ACKNOWLEDGMENTS

I wish to express my appreciation to Dr. Benton W. Buttrey for the cultures and original specimens used in the investigation. In addition, his encouragement, assistance and constant availability for consultation were indispensible.

To the U.S. Department of Health, Education and Welfare, I am indebted for the National Defense Fellowship which provided much of the funding for research.

Finally, I wish to express my gratitude to my wife, Jean, to my son, Eric, and to my parents for their patience, understanding and sacrifices which made this work possible.